Examination of the structural connectivity profile of the Bed Nucleus of the Stria Terminalis in the human brain using probabilistic fiber tracking of diffusion weighted magnetic resonance imaging data

Inaugural-Dissertation
zur Erlangung des Doktorgrades
der Medizin

der Medizinischen Fakultät
der Eberhard Karls Universität
zu Tübingen

vorgelegt von

Krüger, Oliver

2016

Dekan:	Professor Dr. I. B. Autenrieth
1. Berichterstatter:	Professor Dr. T. Ethofer
2. Berichterstatter:	Universitätsprofessor Dr. Dr. F. Schick
3. Berichterstatterin:	Professor Dr. I. Mader

Table of Contents

Abbreviations

ACTH – Adrenocorticotropic hormone

AD – Alzheimer's Disease

ADC – Apparent diffusion coefficient

AMPA – α-amino-3-hydroxy-5-methyl-4-isoxazolepropionic acid

AN – Anorexia nervosa

AVP – arginine-vasopressin

BA – Brodmann's area

BLA – Amygdala, basolateral nucleus

BNST – Bed nucleus of the stria terminalis

BNSTC – Bed nucleus of the stria terminalis, central division

BNSTL – Bed nucleus of the stria terminalis, lateral division

BNSTM – Bed nucleus of the stria terminalis, medial division

CeA – Amygdala, central nucleus

CN – Caudate nucleus

CRF – Corticotropin-releasing factor

DTI – Diffusion tensor imaging

DW – Diffusion weighted

DW-MRI – Diffusion-weighted magnetic resonance imaging

EPI – Echo-planar imaging

FA – Fractional anisotropy

FLAIR – Fluid-attenuated inversion recovery

fMRI – Functional magnetic resonance imaging

GABA – gamma-Aminobutyric acid

HD – Huntington's disease

HPA – Hypothalamo-pituitary-adrenal hormone axis

IPAC – Interstitial nucleus of the posterior limb of the anterior commissure

LH – Luteinizing hormone

MAP – Mean arterial pressure

MD – Mean diffusivity

MeA – Amygdala, medial nucleus

mPFC – Medial prefrontal cortex

MRI – Magnetic resonance imaging

MS – Multiple Sclerosis

NAcc – Nucleus accumbens

N/OFQ – Nociceptin/orphanin FQ

NPY – Neuropeptide Y

OFC – Orbitofrontal cortex

PDF – Probability density function

PET – Positron emission tomography

PFC – Prefrontal cortex

PFT – Probabilistic fiber tracking

PVH – Paraventricular nucleus of the hypothalamus

SI – Substantia Innominata

ST – Stria terminalis

TE – Echo time

TI – Inversion time

TR – Repetition time

VTA – Ventral tegmental area

Preface

The Bed Nucleus of the Stria Terminalis (BNST) is a basal forebrain structure that has been subject to vast research, especially in the last three decades. Repeated investigation of its anatomy, connectivity, and function has provided a multitude of assumptions and theories concerning its role in emotional and hormonal regulation as well as in processing threat and stress, but also in regard of its relevance for the emergence and upkeep of addictive behavior, its involvement in personality disorders, and in further pathologies.
Yet, since most of the anatomical research was conducted on different kinds of animals, little is known about the BNST's structural connectivity profile in humans. In the last years, several studies have investigated functional connectivity to other brain structures in a variety of settings; however, attempts on describing its structural connections have been scarce.

In the *Introduction* to this thesis, a comprehensive overview over the main results of research conducted on the BNST, as well as over the basic principles of diffusion weighted magnetic resonance imaging (DW-MRI) and probabilistic fiber tracking (PFT) is provided.
In *Experiment & Analysis*, results are presented from an investigation of the BNST's connections in living humans. The BNST was identified on high-resolution T_1-weighted magnetic resonance images in order to create seeds for PFT, which was performed on the DW-MRI data sets of 73 healthy participants. Congruence as well as discrepancy of the results with earlier findings from animal studies are discussed.

I Introduction

1 The Bed Nucleus of the Stria Terminalis

1.1 Localization

The Bed Nucleus of the Stria Terminalis (BNST) is a grey matter structure of the basal forebrain. It is positioned on the lateroventral border of the lateral ventricle of the respective hemisphere at the level of the anterior commissure, which it surrounds near its decussation.

Its dorsal, supracommissural part borders (1) medially to the septal nuclei; (2) mediodorsally and rostrally to the lateral ventricle; (3) laterally to the internal capsule; and (4) caudally to the anterior border of the thalamus [167, 280]. Caudodorsally, at level with the border between the thalamus and the corpus of the caudate nucleus (CN), it merges with the stria terminalis (ST), which, along its whole course to the amygdala, sporadically encloses neuron cell bodies, some of which belong to the BNST [100, 149], while others have been identified to relate to different brain structures [7].

The ventral, infracommissural BNST forms a continuum with surrounding grey matter structures, those being (1) rostrally the nucleus accumbens (NAcc) and its transition zone with the CN; (2) rostroventrally and ventromedially the anterior hypothalamus, especially its preoptic area and paraventricular nucleus (PVH); and (3) ventrolaterally the (sublenticular) substantia innominata (SI), which, in addition, contains scattered BNST cell groups extending as far as the amygdala [37, 167, 280]. Furthermore, the ventrolateral BNST blends with cells of the interstitial nucleus of the posterior limb of the anterior commissure (IPAC) [5].

1.2 Microstructure and Immunohistochemistry

Several authors have attempted to differentiate sections of the BNST by various criteria. While in the rat brain the number of described subnuclei excesses 20 [66,

77-81, 191], the human BNST is usually partitioned into three to six divisions with further subdivision depending on the method of examination, e.g. cytoarchitecture [14, 181] or chemo-anatomy/immunohistochemistry [167, 280]. Common to most of these descriptions is a columnar alignment, roughly dividing the BNST into medial, central, and lateral parts. Apart from that, islands of granule cells can be found randomly distributed throughout the entire BNST; those island show close similarity to the insulae terminales [228] or “Islands of Calleja” that are usually located in the NAcc and the basal forebrain (including the olfactory tubercle in non-primates), which are attributed to the reward system and to reproductive functions (for a summary see [257]), and which are suspected to play a critical role in the pathogenesis of schizophrenia [121].

The BNST shows a complex distribution of a multitude of neurotransmitters including dopamine, enkephalin, neuropeptide Y, neurotensin, noradrenaline, somatostatin, substance P, vasoactive intestinal peptide (VIP), vasopressin, and others [98, 167, 271, 280, 288]. Although single BNST subnuclei contain terminals for more than one of these transmitters, they rarely seem to converge onto the same cell [167].

Differences in the internal organization of human versus rodent BNST [167, 288] concern, among others, (1) the value of specific parts of the BNST, e.g. the medial division, which is associated with the accessory olfactory system, and therefore better developed in rodents; (2) the distribution of neurotransmitters, which is much more complex in primates; (3) the morphological similarity to other parts of the so-called “extended amygdala” (vide infra).

As the microstructure of the BNST cannot be examined with routine MRI techniques, it will not be illustrated in further detail in this paragraph. Still, some aspects will be discussed in chapter *1.3 Networks Including the BNST*, page 4, and in the material and methods chapter (see paragraph *3.3.1 Preprocessing of Structural Data and Seed Definition*, page 28).

1.3 Networks Including the BNST

As the anatomical examination of fiber tracts in the brain requires invasive manipulation (e.g. tracer injection, setting of lesions), most of the knowledge on the BNST's role in neural networks is based on experiments performed on animals.

1.3.1 The Extended Amygdala

The BNST is interposed in neuronal circuits belonging to the limbic system. Due to its localization and its close cytological and functional relationship, the complex of amygdala, stria terminalis, its bed nucleus, and other parts of the basal forebrain, is often referred to as the "extended amygdala". Several authors further divide this functional system into two parts [6, 185], namely (1) a central division, consisting of the central amygdalar nucleus (CeA), the lateral BNST (BNSTL), and parts of the SI including the aforementioned scattered BNST cell clusters, as well as the IPAC [8]; and (2) a medial division, consisting of the medial amygdalar nucleus (MeA), the medial BNST (BNSTM) and different parts of the SI. This classification is mainly based on similarities in neuronal composition of the respective nuclei [184], and it has been assumed that the components of the extended amygdala derive from a common anatomical entity (e. g. [66]); in addition, a recent study on human and non-human primates has shown coordinated functional activity of the individual parts during rest [207].

The two most important pathways within this network are the stria terminalis (ST) and a pathway through the ventral basal forebrain.

The ST primarily connects the amygdala and the hypothalamus, but also includes collaterals to the hippocampus, preoptic area, nucleus accumbens, and other parts of the basal forebrain, with numerous interconnections to the BNST [65, 185, 198, 284]. Originating from the amygdala, the ST runs along the roof of the inferior horn of the lateral ventricle, curves around the posterior margin of the thalamus and then accompanies the thalamostriate vein in a groove on the floor of the body of the lateral ventricle, at the border between the thalamus and the body of the caudate nucleus, and finally, on passing through the BNST, splits into

several bundles to reach its target structures in the basal forebrain [22, 67, 106, 149].

The ventral, sublenticular pathway is a more diffuse fiber tract that connects the amygdala and the basal forebrain, including the BNST, through the substantia innominata, incorporating the aforementioned clusters of BNST cells [153, 163, 204]. This direct pathway is frequently referred to as “ventral amygdalofugal/amygdalopetal tract” or “ansa peduncularis” (e.g. [81, 259, 284]). It should be noted that, by some authors, the latter term is also used to summarize three closely related tracts, i.e. the ventral amygdalofugal fiber, the inferior thalamic peduncle and the ansa lenticularis [48]. There is evidence that some of the hippocampus’ influence on the hypothalamus and basal forebrain is communicated via this tract [213].

As mentioned before, some differences in the composition of the extended amygdala have been described in humans versus rodents. While in the human brain there seems to be a close connection between BNSTL and CeA, in the rodent brain it is the central BNST (BNSTC) that’s more closely related to the CeA, whereas the BNSTL shows stronger association with the ventral striatum and with intercalated masses of the amygdala and striatal complex [167, 222].

Although widely accepted, the concept of the extended amygdala is not undisputed. Only recently, Bienkowski et al. [34] found that, although many brain regions project to both amygdala and BNST, only very few neurons innervate both structures at the same time. Nonetheless, a close functional relationship between the parts of this network cannot be denied (see chapter *1.5 Functional Role of the BNST*, page 7).

1.3.2 Further connections of the BNST

Apart from amygdaloid afferents and efferents, the BNST is interconnected with a variety of cortical and subcortical structures.

Of the BNST’s connections to the hypothalamus, those to the paraventricular nucleus (PVH) [80, 81, 192, 198, 231, 233] are of particular interest and therefore will be further discussed in chapter *1.5 Functional Role of the BNST*, page 7

(see, in particular, paragraph *1.5.3 The BNST's Influence on Autonomic Reactions to Stress*, page 10). In addition, the BNST is linked to the preoptic area [65, 77, 79-81, 198] and other, mainly supra- and premamillary parts of the hypothalamus [284]. Moreover, there have been sporadic reports of connections to the thalamus [81, 240].

Experiments in animals have shown strong coupling of the BNST, for example via the medial forebrain bundle [128], with the ventral tegmental area (VTA) [102, 103, 137, 157] and several brainstem regions, such as the nucleus of the solitary tract [16, 19, 77, 220], the dorsal vagal complex [108], and the parabrachial nucleus [16, 116, 229]; a detailed description of the BNST's brainstem connections in the cat was provided by Holstege et al. [128]. The significance of these interdependencies will also be accounted for in following chapters of this thesis.

Cortical regions that have been reported to be associated with the BNST include parts of the hippocampus, mainly the ventral subiculum [40, 41, 185, 198], the insular cortex [143, 185, 240], and the medial prefrontal cortex (mPFC), more precisely the infralimbic cortex [185, 240, 260, 273] and, to a much lesser extent, the prelimbic cortex [131, 185].

1.4 Sexual Dimorphism of the BNST

Some authors have reported gender differences concerning the size of the BNST, with the BNST in males being larger and containing more neurons than in females [9, 10, 156, 293]. In rodents, this applies especially to divisions of the BNST (e.g., the so-called encapsuled region of the BNST; arginine-vasopressin (AVP) neurons) that are interconnected with other sexual dimorphic structures of the brain (e.g., the sexually dimorphic nucleus of the preoptic area) and that show pronounced response to gonadal hormones in comparison to other BNST regions [125, 188, 272]. However, these conclusions may not be uncritically transferred to the human brain, as, for example, AVP innervation of the limbic system,

including the BNST, has been shown to be much less intense and to exhibit no sexual dimorphism in humans [92].

While in rodents sexual dimorphism already occurs at a young age [52, 70], it only gains significance in adult humans, i.e. the male BNST continues to grow into adulthood while growth of the female BNST comes to a halt in adolescence [52]; this difference cannot solely be ascribed to hormonal differences during development, as, for example, testosterone levels of females and males already differ in the perinatal period [1]. On the other hand, changes in gonadal hormone levels seem to have no effect on BNST growth after reaching adulthood [156, 293]. There has been evidence suggesting that in transsexuals, the size of the BNST corresponds to the gender that the respective person feels related to [156, 256, 293]. Yet, to this day, the significance of these differences remains unclear.

1.5 Functional Role of the BNST

As a part of the limbic system, the BNST is mainly involved in processing emotional information and has a strong influence on a variety of the brain's and body's reaction especially to (emotional) stress, but it is also assumed to be involved in sexually motivated behavior like mating or male aggression.

It furthermore plays a role in reward systems and therefore in the development and upkeep of substance dependence, as well as in drug relapse. This dysfunctional aspect will be discussed in a following chapter about the BNST's involvement in pathological processes (see paragraph *1.6.1 The BNST's Relevance to Substance Dependence*, page 14).

1.5.1 The BNST's Role in Phasic vs. Sustained Fear

The extended amygdala complex is one of the brain's main functional circuits in expressing fear and anxiety in the presence of aversive stimuli, and several experiments have attempted to dissect the role of its particular structures.

A repeatedly used setting in the investigation of this paradigm is the potentiation of startle reactions under varied circumstances. For example, rodents react with increased startle to a loud sound, when it occurs shortly after a stimulus (e.g. a light flash) that has earlier been conditioned to an aversive event (e.g. electric

foot shock). Inactivation of the CeA, but not of the BNST, by injection of an AMPA antagonist significantly reduces this effect. At the same time, these animals exhibit increased startle to loud sounds when kept in a brightly illuminated environment [276], a condition that is considered menacing for prey animals; this effect is dramatically decreased in animals that received preceding injections of AMPA antagonists into the BNST, while injection of AMPA antagonists into the CeA has no significant effect on this so-called light-potentiated startle reaction [63, 277]. Meanwhile, injection of AMPA antagonists into the basolateral nucleus of the amygdala (BLA) decreases startle reaction in both cases, as the BLA densely projects to both CeA and BNST [154]. Initially these results were interpreted in a way that the amygdala is responsible for threat conditioning, while the BNST processes unconditioned fear. Yet, it later has been suggested that the amygdala is essential for responses to immediate (phasic), explicit danger whereas longer-lasting (sustained), less specific (contextual) threats elicit BNST activation [85, 254, 278, 279]. This assumption coincides with results from a micro-PET examination in rats that revealed heightened metabolism in a cell cluster comprising the BNST and adjacent structures in a rat model of contextual anxiety, both in comparison to normal controls, as well as to rats with cued fear [174].

Several authors have proposed that contextual anxiety is mediated by the stress hormone corticotropin releasing factor (CRF). This theory is supported by observations that CRF injections into the BNST and the ventricles increase contextual startle reactions [160], while CRF antagonists block CRF-enhanced startle [62] and freezing [68, 142]. At the same time, CRF injection into, or CRF blockade in the CeA, as well as lesions to the CeA, do not influence CRF-enhanced startle [160]. These findings further confirm assumptions on the amygdala's and BNST's role in phasic versus sustained fear.

In the last years, a couple of studies also addressed this issue in humans, mostly by examining brain activation in different contexts of threat and fear with methods of functional magnetic resonance imaging (fMRI). A study by Herwig et al. [124] showed greater activation of the BNST (and other brain regions) while expecting negative events in contrast to neutral events. Moreover, BNST activity correlates

with the level [64] and proximity [190, 246] of a possible threat. Investigation of the BNST's and amygdala's activation in predictable versus unpredictable threat revealed incoherent findings; while both structures respond to unpredictable threat, Alvarez et al. [11] did not observe significantly heightened BNST activation during predictable conditions, whereas Choi et al. [50] found stronger activation of the BNST during the cue phase of threat relative to safety.

1.5.2 BNST and Trait Anxiety

The effect of the BNST on anxious reactions varies inter-individually and is suspected to play a role in a number of psychiatric disorders.

In rats, blockade of GABA synthesis in the BNST, and therefore of its inhibitory outputs, results in behavior much alike general anxiety disorder in humans, but very distinct from panic [227]. In contrast, lesions to the BNST decrease contextual anxiety and lead to behavior, which strongly resembles that of animals of the non-anxious phenotype [85].

In monkeys, anxious temperament has been shown to correlate with the activity of a brain circuitry including amygdala, BNST, hippocampus, and periaqueductal grey [94], and the availability of serotonin transporters in several of these structures appears to be of particular importance to trait anxiety [206]. The latter finding coincides with considerations of serotonin in the BNST having a predominantly anxiolytic effect [117, 168], and offers a possible explanation for increased anxiety in major depression. However, it is not clear how this influence is conveyed, since recent research indicates that activity in the anterodorsal and anterolateral subdivisions of the BNST actually provides several features of anxiolysis [111, 148], meaning that the BNST is not only involved in eliciting, but also in suppressing anxious states.

Straube et al. [253] elaborated that the increase in BNST activation in the expectation of aversive events vs. neutral events [124] is even more remarkable in phobics than in non-phobics. Furthermore, brain reactions to threat proximity [246], as well as to longer-present threats [110] seem to depend on levels of anxiety, with the BNST playing an important role in *"maintaining persistent states of heightened anxiety"* [247]. Yassa et al. [291] hypothesized that in patients with

general anxiety disorder, this state of maintenance, and therefore involvement of the BNST in processing a potentially harmful situation, is reached much earlier than in non-anxious persons.

Interestingly, although personality traits are widely believed to be consistent within an individual over time, chronic stress, both in the form of social isolation and of chronically elevated corticosterone levels, leads to an increase in anxiety-like behavior and, via neuroplasticity, to impairment of long-term potentiation in parts of the BNST [56]. These findings do not necessarily challenge the principle of personality stability, but they might lead to new insights in the neural correlates of anxiety disorders and other psychiatric illnesses, particularly with regard to the BNST.

1.5.3 The BNST's Influence on Autonomic Reactions to Stress

Both physical and mental reactions to stress are, to a great part, mediated by the hypothalamo-pituitary-adrenal hormone axis (HPA). The HPA is predominantly controlled by the paraventricular nucleus of the hypothalamus (PVH), which integrates inputs from a variety of stress-processing systems and generates autonomic, behavioral, and hormonal responses [123, 234] by secretion of CRH and arginine-vasopressin, two adrenocorticotropic hormone (ACTH) secretagogues, into the pituitary portal circulation [286].

One major source of information influencing the PVH is the medial prefrontal cortex (mPFC), which mainly modulates and suppresses PVH responses [91, 270]. Surprisingly, examinations of the rat brain found no evidence of an explicit connection between these two structures [93]; similar observations concerning connectivity to the PVH have been made regarding the amygdala [216].
As a result, the BNST with its repeatedly described connections to the PVH [80, 81, 192, 198, 231, 233] and its central position has been discussed to be a possible relay in the interdependency of these structures. Earlier studies on rats have already shown fiber tracts that originate in the prelimbic [260] and, to a lesser extent, in the infralimbic [131] area of the mPFC, to innervate the BNST. Moreover, mPFC lesions that led to increased PVH activity at the same time led

to altered neuronal recruitment in the BNST, but not in other examined regions of interest [248]. Also, lesions to the dorsal mPFC and selective lesions to GABAergic neurons of the anterior BNST had a similar effect on CRH mRNA and Fos (a neuronal activity marker) expression in the PVH [218].
An examination in monkeys revealed only few direct connections of mPFC and BNST, but dense mPFC projections to the ventromedial CN and the NAcc [47]; the latter has already been shown to relate to the stria terminalis and its bed nucleus (vide supra). A pathway between the CN and the BNST, to the author's knowledge, has not yet been described; however, the results from the study described in *II Experiment and Analysis* in this thesis suggest the existence of a fiber tract between prefrontal cortex regions and BNST that courses, amongst others, through the head of the CN (see chapter *5.2 Connections via the Anterior Projection*, page 43).

Further inputs to the BNST that affect HPA activity arise from various brainstem regions (e.g. the nucleus of the solitary tract, the ventrolateral medulla, and the lateral parabrachial nucleus); they are, for example, assumed to increase HPA activity in illness, more precisely in the presence of bacterial endotoxin [33]. Hypoxia leads to increased Fos expression in BNST regions connected to the ventrolateral medulla [126], and there has been evidence suggesting a role of the BNST in the dysregulated ACTH response to stress in patients with obstructive sleep apnea [175]. Moreover, BNST subnuclei show increased activity in response to both acute and chronic pain [194, 224], and they are involved in developing pain-related place aversion [133], as well as pain-associated decrease in food-intake [199]. Meanwhile, inhibition of noradrenaline release in the ventral BNST [76] and injection of neuropeptide Y into the BNST [133] suppress pain-induced aversive behavior.

Most of the BNST's neurons have been shown to provide GABAergic output [60], and therefore its impact on the PVH and the HPA is supposed to be mainly inhibitory. Still, the BNST also sends some CRH and glutamate projections to the PVH, indicating an activating effect of some BNST cells on the PVH [192]. Choi et al. [49] suggested spatial differences in BNST influence on the PVH, with

posterior nuclei being inhibitory, whereas anteroventral nuclei seem to be involved in HPA axis excitation; yet, data concerning this matter is inconsistent (cf. [83, 109, 122, 218]).
Additionally, some fibers reciprocally project from the PVH to the BNST, and there is evidence that they are part of a feedback loop between the hypothalamic oxytocin system and the forebrain CRF system [61].

Apart from its influence on the PVH, the BNST is furthermore involved in the regulation of other stress-processing networks. Projections to the parabrachial nucleus [116, 191] affect cardiovascular function; in this context, stimulation of the BNSTM has been shown to increase mean arterial pressure (MAP), while stimulation of the BNSTL reduces MAP [84]. BNST-mediated changes of MAP and heart rate especially occur under emotional stress and during physical exercise [58]; the exact underlying mechanisms are complex, though, and several aspects remain unclear to this date (for a comprehensive review see [59]).
Moreover, Simerly et al. [244] found high numbers of sex hormone receptors in the BNST, with androgens presumably leading to increased HPA activity [35]. A role of the BNST in the suppression of pulsatile secretion of luteinizing hormone (LH) as a result of stress has initially been estimated unlikely [221], but was recently re-assumed [171].

1.5.4 Influence of the Extended Amygdala on Sexual Functionality

In several studies, a role of the extended amygdala and the BNST in reproductive behavior of male rodents has been observed. Electric stimulation of the lateral preoptic area, BNST, and neighboring structures evoked penile erection in both wake and anesthetized male rats [135]. Lesions to the BNST led to slower initiation of copulation, to prolonged intervals between intromission and ejaculation, and to more intromissions preceding ejaculation, in some cases even failure in ejaculating [87, 269]. Some animals, who received particularly large lesions, even showed complete abandonment of mating activity. A role of BNST neurons in this matter could not be clarified definitely, as lesions to the stria

terminalis evoke equal effects [164, 212]. Still, regions of the medial extended amygdala (i.e. the CeA and the encapsuled region of the BNST) that show extensive uptake of gonadal hormones, are much larger in male than in female rats [125], and therefore are candidates for mediating these behaviors.

As stated above, parts of the BNST associated with the olfactory system are much more developed in the rodent brain than in humans, and there have been multiple reports of rodents being highly dependent on olfactory stimuli, especially those perceived by the vomeronasal organ, when it comes to initiating copulation and further sexually oriented behavior, and lesions to parts of the olfactory system have been shown to lead to a radical decrease in sexual interest, too (e.g. [45, 75, 215, 287]). The medial and accessory olfactory bulb both send direct projections to the MeA and the BNST, implying their involvement in this cascade [258].
It is questionable, whether a role of the BNST in processing this kind of signals is significant in humans. Still, even in rhesus monkeys, a striking effect of pheromones on sexual attraction has been observed [187], and only in recent years, an influence of odors produced by humans on sexual attraction [172], as well as on activation of the limbic system [173], has been shown.

Furthermore, it has been demonstrated that human female pheromones affect the ovulatory cycle of other women [250], sometimes possibly even leading to menstrual synchrony [136, 285] in women sharing a lot of time in the same places (e.g. co-workers, roommates), and these effects are thought to be mediated by changes in the pulsatile secretion of LH [241]. Regarding the BNST's possible role in processing vomeronasal and olfactory stimuli and its probable impact on LH secretion (as already mentioned in paragraph *1.5.3 The BNST's Influence on Autonomic Reactions to Stress*, page 10), it might therefore again be a possible relay for integrating and transducing these signals. Still, to the author's knowledge, there has yet been no research addressing this relationship, which thus remains merely hypothetical.

1.6 BNST Involvement in Pathological Processes

In addition to possible pathological imbalances in the abovementioned systems, the BNST has been shown to be involved in a number of illnesses und dysfunctional processes related, among others, to the limbic or reward system. In most cases, it has not yet been possible to clarify if those pathologies are only mediated via the BNST, or if some of them actually originate there. Still, the findings to be discussed corroborate the theory of the BNST being a highly important center in in the integration of information arriving from multiple brain systems.

1.6.1 The BNST's Relevance to Substance Dependence

Amygdala and BNST play an important role in perpetuation of drug misusage, as they are thought to be involved in the affective state of drug withdrawal [200], which is mediated by inputs of CRF [252] and noradrenaline [19, 71]. Drug withdrawal leads to an increase in BNST CRF levels [208], especially after stressful events [89, 166], eliciting augmented signaling towards the VTA [243], a key region for drug-seeking behavior [255] and drug-related place preference [118]. Thus, interruption of BNST-to-VTA projections has been shown to significantly attenuate expression of cocaine preference in rats [232]. Furthermore, reversible deactivation of the BNST reduces reinstatement of cocaine seeking in response to stress [237] as well as in response to re-exposure to cocaine itself [39]. Meanwhile, injection of β_1- and β_2-antagonists into the BNST only has an inhibiting effect on reinstatement due to stress [166], but at the same time decreases withdrawal-induced place aversion [19]. Additionally, injecting a $GABA_A$-inhibitor reduces motivated responding for alcohol (i.e. voluntary consumption) in rats [132].

Another brain region that appears to play an important role in the upkeep of substance consumption and in drug withdrawal is the insular cortex, which is thought to be crucial for mediating subjective awareness of interoceptive information and thus of visceral changes during drug withdrawal [107, 202]. Connections between BNST and insular cortex have previously been described

[143, 185, 240], and therefore interplay of these structures in the context of substance dependence and especially drug withdrawal appears to be likely. Since these projections appear to run mainly unidirectionally from the insula to the BNST [219, 230] (see [6] for exceptions), the BNST might, at least partially, integrate information from the insular cortex with inputs from further brain regions involved in drug withdrawal. However, to the author's knowledge, there have not been any studies investigating this relationship, yet.

Finally, the BNST has been ascribed a role in communicating the rewarding effects of substance consumption [86, 88], mainly elicited by dopamine input into the BNST. Still, this effect does not seem to be specific to the consumption of drugs, as in rats, increased dopamine levels and (at the same time) decreased noradrenaline levels in the BNST have also been observed in response to other pleasing substances, such as sucrose [178, 210]. Moreover, Park et al. [210] reported a reciprocal effect (i.e. a decrease in BNST dopamine levels and an increase in noradrenaline levels) when administering quinine, a substance of unpleasant taste, but in this case, the effect seemed to arise more slowly and to last longer. Park and colleagues [210] therefore reasoned that the BNST is involved in the integration of reward and aversion in a way that allows fast retrieval in the context of a pleasant stimulus, while aversive stimuli are continuously avoided. When further investigating this hypothesis, Park et al. [211] observed increased dopamine levels in the dorsolateral BNST following a cue predicting reward, whereas increases in ventral BNST norepinephrine levels were seen as a result of the sudden absence of anticipated pleasant stimulation. These findings point towards a differential distribution of oppositional functions across BNST subnuclei. Finally, Choi et al. [51] described increased activity of the human BNST, measured by fMRI, in both threat and reward, arguing for inter-species congruence.

1.6.2 A Possible Role in Eating Disorders

In rats, BNST activity has been shown to increase when anticipating feeding [15], and its connections to the lateral hypothalamus are thought to be involved in

feeding regulation, as the lateral hypothalamus is regarded as the essential brain area in inducing food intake [12, 72]. In a recently conducted study, Jennings et al. [139] demonstrated that activation of BNST inhibitory projections to the lateral hypothalamus dramatically increases food intake even in well-fed mice, that those animals develop a striking preference for places where this stimulation occurs, and that they especially prefer high-fat food. Meanwhile, inhibition of this pathway leads to reduced feeding and to avoidance of places where inhibition occurs.

On the other hand, the BNST is also discussed to be involved in anorexia nervosa (AN), as CRF injected into the cerebroventricular system or selectively into the BNST leads to reduction in food intake [53, 54], an effect that can be prevented by precedent injection of the anti-stress transmitter nociceptin/orphanin FQ (N/OFQ), an agonist at the opioid-receptor like receptor ORL-1, into the BNST [54]. Meanwhile, injection of N/OFQ alone (i.e. without previous injection of CRF) does neither influence food intake [55], nor inhibit HPA activity [74]. However, these observations have to be interpreted carefully, since more recently, a study in humans showed that deactivation of the NAcc, both through lesions as well as deep brain stimulation, leads to complete abandonment of anorectic behavior as well as to improvement of AN-associated personality aberrations [281]. It therefore has to be considered that the abovementioned injections of CRF or N/OFQ directly influenced the NAcc as well. Still, since the NAcc has been shown to be anatomically connected to the BNST (vide supra), these two structures might both contribute to the observed effects.
In summary, these findings reveal a possible role of the BNST in extreme forms of pathological eating behavior, i.e. both in morbid obesity and pronounced AN.

1.6.3 BNST in Neurodegeneration

Like many other brain regions, the BNST is affected by neurodegenerative diseases, whereas its role in generating typical symptoms of these disorders is hardly examined.

In animal models of Alzheimer's disease (AD) [38] and in human AD patients [182], HPA activity has been shown to be increased, and elevated amounts of CRH mRNA in the BNST have been reported [120]. Moreover, in an animal model of AD, reduced immunoreactivity of neuropeptide Y (NPY) in BNST, NAcc, CeA, arcuate nucleus, and dentate gyrus has been observed, with restitution to normal levels (compared to healthy animals) under treatment with nicotine. However, and even though NPY-reduction in cerebrospinal fluid of AD patients correlates with clinical characteristics and duration of illness [189], no significant difference in BNST immunoreactivity to NPY between AD patients and controls has been shown in the human brain [99]. Finally, norepinephrine in the BNST supposedly plays a role in the acquisition of spatial memory [46], a mechanism that, when disturbed, could be relevant for the development of spatial disorientation in AD.
In Huntington's disease (HD), on the other hand, an increase in NPY, with an extent proportional to the pathological grade, has been reported in the BNST [29], while substance P immunoreactivity [28] and dopamine D2/3 receptor binding [214] are diminished. Additionally, microglial activity, which is thought to lead to neuronal death, and whose extent correlates with clinical scales of the disease [201], is elevated [214]. Furthermore, mRNA for Huntingtin-associated protein HAP1 is highly expressed in parts of the limbic system, including the BNST [209]; this might contribute to HD patients' problems in recognizing facial expressions, especially negative ones [158], and possibly to the development of aggressive behavior that is typical for advanced HD [183].

When regarding these changes, it has to be kept in mind that similar signs of degeneration have been found in several further brain regions. Therefore the question remains, whether affection of the BNST is of relevance for the respective illness's pathogenesis and symptomatology, or merely a byproduct of the neurodegeneration process.

1.7 Conclusion

In summary, it has to be pointed out that the BNST appears to be an important structure in ensuring survival, (1) from a behavioral point of view, by promoting

avoidance in the face of possible threat, as well as through its role in the initiation and execution of mating behavior, and (2) with its influence on autonomic reactions, i.e. by eliciting somatic reactions to stress, both acutely, via its influence on various brainstem nuclei involved in the regulation of cardiovascular function, and continuously, by directly acting upon the PVH, the key impulse generator for the hypothalamo-pituitary-adrenal axis. Since the BNST is a very heterogeneous structure, it is commonly assumed that these functions are carried out by different subnuclei, respectively, and only in the last years, research has aimed at dissecting the BNST not only into histological, but also into functional subdivisions. Gaining further information on its exact functionality is crucial in order to then investigate its possible role as a target in the therapy of a variety of mostly psychiatric illnesses, such as anxiety disorders and substance dependence. In this context, examination of inter-species differences has to be pressed ahead. Both BNST anatomy and functions feature essential differences between species, and knowledge in humans is limited and often non-specific. The anatomy of the human BNST has only been investigated in the brain of deceased persons, and its structural connectivity profile is practically unexplored. Most research on the BNST's functions in the human brain is based on fMRI, and therefore only allows statements about the BNST in general, since fMRI resolution is much too low to display the different compartments of the BNST. It has furthermore not yet been possible to determine, which transmitters are involved in what kind of task, what brain regions provide direct input to the BNST, and what its target areas are. Hopefully, advancements and innovations in imaging techniques such as MRI, PET, and nuclear medicine will provide more detailed insights on these questions in the future. Results from a study aiming at displaying the BNST's structural connectivity profile using a relatively new approach based on probabilistic fiber tracking of diffusion-weighted magnetic resonance imaging data will be presented and discussed in *II Experiment & Analysis,* page 27.

2 Diffusion Weighted Imaging and Probabilistic Fiber Tracking

2.1 General Ideas behind Diffusion Imaging

Diffusion-weighted magnetic resonance imaging (DW-MRI) is a technique in magnetic resonance imaging (MRI) that allows depicting diffusivity properties of tissues. In DW-MRI, signal intensity depends on the average distance that a water molecule travels in the direction of a gradient field in a defined period of time; the farther the molecule travels, the greater the loss of signal [283]. While in isotropic media the degree of this effect is independent from the direction of the gradient, in anisotropic media (i.e. media, in which diffusion is more probable in some directions than in others, e.g. brain white matter) the degree of signal decrease depends on the direction of the gradient.

Discoveries in the 1950s first allowed spin-echo [43, 115], then pulsed-gradient spin-echo [249] measurement of scalar diffusivity in isotropic media. Later, combination with Fourier MRI [186, 261] allowed estimation of effective scalar diffusivity in the single voxels of an image. However, as already mentioned, calculation of this scalar diffusivity in anisotropic media leads to different results depending on the direction of the diffusion gradients.

2.1.1 Diffusion Imaging Sequence

The sequence used to acquire diffusion-weighted data is a variation of the pulsed-gradient spin-echo sequence [4, 283].

First, a 90° high frequency impulse is applied, which causes the spins of the tissue's protons to precess about the constant magnetic field B_0 at Larmor frequency.

It is then followed by a pulsed field gradient that slightly changes Larmor frequency in a degree depending on the proton's exact position, causing the beforehand synchronously precessing flipped spins to dephase. The direction of this gradient is the direction in which diffusivity is measured. In order to receive optimal results, the pulsed field gradient has to be both of high strength (G) and short duration (δ) [267].

Next, a 180° refocusing pulse is applied and finally, spins are rephased using the same pulsed field gradient as before. Spins in stationary molecules are completely rephased and therefore all their signals add up constructively, providing a high intensity signal. Meanwhile, molecules that diffused between the two gradient impulses show a net phase difference, which is proportional to (1) the amount of displacement in the direction of the gradient, (2) the amplitude of the dephasing pulse *G*, (3) the pulse's duration *δ*, and (4) the time *Δ* between the two gradient pulses; G, δ, and Δ define the *b-value* that specifies the measurement's sensitivity to diffusion [159]:

$$b = \gamma^2 G^2 \delta^2 (\Delta - \frac{\delta}{3}),$$

with γ being the gyromagnetic ratio. Readout is then carried out as usual.
In honor of the pioneer work performed by E.O. Stejskal and J.E. Tanner, this method is commonly referred to as the "Stejskal-Tanner sequence".

2.1.2 Error Minimization

As different properties of the examined media lead to different signal answers per se, and furthermore to distortion of the magnetic field, to evaluate a diffusion weighted data set correctly, acquisition of and comparison (by coregistration) to another data set with a b-value of 0 s/mm² (i.e. a non-diffusion weighted data set) is necessary. Furthermore, to reduce statistical noise, it is advisable to measure more than one set of diffusion weighted images and then average across sessions.
As DW-MRI is very sensitive to every kind of motion, even to pulsations of the blood flow, the use of motion-insensitive sequences like single-shot EPI that provide very short echo and read-out times is favored [203, 266, 267]. Still, other sources for artifacts remain, such as image warping as a result of eddy currents that are induced in conducting parts of the MRI scanner by rapid switching of the applied gradients, leading to unwanted magnetic field distortions that violate the integrity of the desired magnetic field; these effects can be reduced using prospective (e.g. by image acquisition with bipolar gradient pulses, see Bar-Shir et al. [23]), retrospective (for example by coregistration to T2-weighted images,

e.g. as described by Techavipoo et al. [262] or Mohammadi et al. [193]), or combined [289] techniques.

2.1.3 From Diffusion Weighted Images to Diffusion Tensors

As noted above, the measured extent of diffusion in anisotropic media depends on the direction of the dephasing gradient; to get a more accurate idea of diffusivity, specification of a diffusion tensor, which contains information on diffusivities along different axes, is necessary. In anisotropic media, estimation of the diffusion tensor requires a minimum of six diffusion weighted (DW) acquisitions in non-collinear diffusion encoding directions and an additional non-DW image (b = 0 s/mm²) [242], or seven DW acquisitions in non-collinear encoding directions [24, 25]. Various suggestions to further improve estimation of diffusion properties have been made, e.g. by measuring each of these directions with multiple b-values [140], by combining tetrahedral and orthogonal gradient encoding [57, 239], or by using a much higher number of encoding directions [129, 144]. To get accurate information on diffusion parameters and at the same time keep disturbances and errors at a minimum, acquisition with at least 20 to 30 gradient directions [141] at a uniform angular sampling [119] has been recommended.

The acquired data is usually processed as follows: First, corrections for movement, magnetic field inhomogeneity, and eddy currents (e.g. [151, 294]) have to be applied. Subsequently, apparent diffusivity maps are calculated for each encoding direction [4]. Signal attenuation for anisotropic diffusion is described by

$$S_i = S_0 e^{-b_i D_{i,app}},$$

where S_i is the DW signal in the *i*th encoding direction, S_0 is the signal without diffusion weighting, b_i is the b-value of the applied gradient in this direction, and $D_{i,app}$ is the apparent diffusivity in this direction.

This expression can be generalized using the diffusion tensor $\boldsymbol{D}$ and the unit vector $\hat{g}_i$ of the DW encoding direction:

$$S_i = S_0 exp^{-b\hat{g}_i{}^T \boldsymbol{D} \hat{g}^i}$$

Subsequently, the independent elements of the diffusion tensor can be estimated from the apparent diffusivity maps by multiple linear least square methods [119, 150] or nonlinear modeling techniques [24].

The diffusion tensor

$$\boldsymbol{D} = \begin{bmatrix} D_{xx} & D_{xy} & D_{xz} \\ D_{yx} & D_{yy} & D_{yz} \\ D_{zx} & D_{zy} & D_{zz} \end{bmatrix}$$

is a 3×3 covariance matrix with symmetric off-diagonal elements (i.e. $D_{xy} = D_{yx}$, $D_{xz} = D_{zx}$, *and* $D_{yz} = D_{zy}$), and its eigenvectors (ε_1, ε_2, and ε_3) represent the tissue's three orthotropic axes, while the corresponding eigenvalues (λ_1, λ_2, and λ_3) carry information about effective diffusivities in the eigenvectors' directions. Originally, the eigenvector belonging to the highest eigenvalue (i.e. the principal eigenvector, ε_1) has been proposed to correspond to fiber-tract axis [25], while the two smaller eigenvectors were interpreted as measurements of diffusion perpendicular to the fiber. Yet, this idea does not sufficiently account for voxels with crossing fibers; this issue was addressed later in the search for reliable fiber tracking methods (vide infra). Both eigenvectors and eigenvalues can be summarized in a diffusion ellipsoid that depicts both main diffusion direction and mean diffusivities, and the eigenvalues can also be used to describe invariant diffusion properties that are independent from tissue orientation and thus help to differentiate between tissue types and to detect microstructural changes.

2.2 Probabilistic Fiber Tracking

The idea of using diffusion tensor imaging (DTI) to display fiber connections in the brain is based on the principle that water diffuses almost freely along the axons and dendrites of nerve cells, while perpendicular diffusion is restricted by the cell membrane, neuronal filaments, and glial cells [4, 30]. General diffusion properties are therefore characterized by three parameters: (1) the apparent diffusion coefficient (ADC), or mean diffusivity (MD), which describes how freely water molecules diffuse in a voxel without regarding the direction of diffusion; (2)

the main direction of diffusion; and (3) fractional anisotropy (FA), which specifies how pronounced the directionality of this diffusion is [26, 195].

MD and FA can be calculated from the diffusion tensor's eigenvalues as follows [26]:

$$MD = \frac{\lambda_1 + \lambda_2 + \lambda_3}{3}$$

and

$$FA = \sqrt{\frac{3}{2}} \sqrt{\frac{(\lambda_1 - MD)^2 + \lambda_2 - MD)^2 + (\lambda_3 - MD)^2}{{\lambda_1}^2 + {\lambda_2}^2 + {\lambda_3}^2}}$$

For uniaxial diffusion ($\lambda_1 > 0$; $\lambda_2 = \lambda_3 = 0$), FA takes a value of 1, while it equals 0 for isotropic diffusion (i.e. $\lambda_1 = \lambda_2 = \lambda_3$).

By many authors, a high value for FA is interpreted as a sign of high white matter integrity, which again is thought to correlate with mental and intellectual performance (e.g. [69, 130]). Correlation with personality traits was also assumed, but could not be confirmed [290].

2.2.1 Early Fiber Tracking Methods

In order to depict whole nerve tracts though, it is not sufficient to be able to predict diffusive behavior in a single voxel; a method is needed that lines up voxels that are likely to contain parts of the same fiber bundle. Early fiber tracking approaches, such as the diffusion tensor model (e.g. [25]), only considered a voxel's main diffusion direction, i.e. the principal eigenvector of the diffusion tensor, to then look at the voxel following in this very direction. Depending on the angle between the principal eigenvectors of those voxels and their respective FA, a decision then had to be made whether tracking should be commenced or stopped. In order to reduce the chance of false positive results, strict confinements had to be made regarding these angles (at a maximum of around 45°) and FA (usually thresholded between 0.2 and 0.4) [251], making it almost impossible to track fibers with a strong curvature, or in areas with low FA, either due to a relatively high content of non-fibrous structures (e.g. the thalamus, the

cerebral cortex), or due to fibers arriving from and/or leaving in various directions (e.g. in parts of cerebellar peduncles near the midline).

2.2.2 First Attempts at Probabilistic Fiber Tracking

A suitable solution for these disadvantages was provided with the introduction of probabilistic fiber tracking (PFT) [31], an approach that generates reliable results even in regions with low FA as well as in branching fiber tracts, and that accounts for the possibility of crossing fibers. One basic principle underlying PFT is to consider a degree of uncertainty in the estimated diffusivity model of each voxel. This is accomplished by creating probability density functions (PDFs) that take into consideration all influencing parameters (depending on the exact kind of approach, e.g. the coordinates of the eigenvectors, the eigenvalues, the signal strength of the measurement without diffusion gradients, and the standard deviation of the signal's noise), feeding them into a Bayesian network, which is then solved using a computational algorithm, for example a Markov chain Monte Carlo method (e.g. [104]). As a result, the uncertainty in the principal eigenvector's angle (within a confidence interval) of the respective voxel is obtained.

To then receive global connectivity profiles, again, a complex probability model has to be set up, which cannot be solved explicitly, but narrowed with high confidence using a sampling technique that draws samples for the principle eigenvector's direction out of the seed voxel's PDF. The front of the so-called probabilistic streamline is then moved a given distance in this direction, thus defining the next voxel of the streamline, where this process is repeated with a sample out of this new front voxel's PDF, and so on, until a termination criterion is met. Subsequently, this algorithm is started over and over again in the seed voxel, usually several thousand times, each time creating a new probabilistic streamline. Finally, the probability of every voxel to be connected to the seed voxel can be viewed as the number of probabilistic streamlines passing through this specific voxel divided by the total number of created streamlines.

One major advantage of this method is the fact, that distal to voxels with high uncertainty, the distribution of streamline voxels will be widespread with low

probabilities for every single voxel. Thus, on the one hand, false positives become less likely, while on the other hand, connectivity of the seed voxel to a region would still be traceable, even if the exact connection path cannot be determined. In that way, PFT allows for much more permissive stopping criteria regarding FA and kinking of streamline direction.

2.2.3 Optimizing PFT Methods

Still, further improvements to this so-called single-fiber approach were necessary in order to retrieve reliable information in brain regions where there is not only one, but two or more main directions of diffusion, i.e. structures containing different fiber tracts on a small space, like the auditory and optic radiation near the geniculate corpora. In 2007, Behrens et al. [32] introduced a modified version of their earlier described concept, this time using PDFs that allow for more than one direction of diffusion. However, since application of such functions to structures with one single predominant direction of diffusion would diminish performance and lead to disturbances in tractography results, a method has to be found which guarantees that these functions are only used when data suggests more than one possible pathway. Therefore, an automatic relevance determination [177] is applied to the Bayesian network, which zeroes parameters that are not supported by the available data. Thus, at a b-value of 1000 smm^{-2}, even when measuring diffusivity in 60 different directions, a maximum of two relevant diffusion directions per voxel is acquired [32].

Fiber tracking is performed similar to the way explained above, now using the newly introduced PDFs for multiple diffusion directions. First, at each new voxel of the streamline, implausible directions are eliminated. What is left is a set of probability functions for each remaining (plausible) direction, from which, again, a sample has to be drawn. There are different possible ways to do so, two of the most obvious being (1) to draw from the whole set, with ascribing the highest chance of being drawn to the probability function of the main diffusion direction (i.e., in the majority of cases, the PDF of the principal eigenvector of the diffusion tensor), or (2) to draw from the set whose direction aligns the most with that of the already existing part of the respective streamline. It is evident that the former

way would be likely to produce results that resemble those of the single-fiber approach, and that it would hardly solve the problems of tracking smaller fiber structures in the vicinity of larger bundles. The latter, on the other hand, proved to be much more reliable than the single-fiber approach when tracing smaller, non-dominant projections, while results for large, dominant projections were alike [32].

2.2.4 Limitations and Suggested Improvements

There are still considerable limitations to this technique. Some fiber tracts can only be depicted with high inter-individual variance, possibly because of a third diffusion direction that could only be detected by automatic relevance determination, if diffusion was measured in even more directions, and especially at much higher b-values. Furthermore problematic are situations in which a non-dominant projection runs approximately parallel, or even immediately adjacent, to a much larger fiber tract (for example projections that contribute to the anterior commissure). In the latter case, it would be almost impossible, even at a much higher resolution, to separate different projections after their coalescence.

There have been further attempts to optimize fiber tracking, especially in voxels with crossing fibers, for example through estimation of fiber orientation distribution functions, rather than discrete diffusion directions, by constrained spherical deconvolution [263, 264], by using q-ball imaging [146, 265], diffusion spectrum imaging [282], or the CHARMED model [18]; for an overview over recent developments see Vos et al. [275]. However, those techniques are mostly complex, with a variety of assets and drawbacks, and describing them in detail would go beyond the scope of this thesis.

Nevertheless, the discussed probabilistic algorithm proves to be very reliable with a high reproducibility, while at the same time requiring only average technical equipment, measurement time and computation power, thus turning out to be highly applicable for clinical use and research.

II Experiment & Analysis

3 Material and Methods

3.1 Participants

Data was acquired from 82 participants; nine datasets were afterwards excluded from analysis due to subject movement in the scanner or other exclusion criteria (i.e. history of psychiatric or neurological disease, present medication). Analysis was performed on data from 73 participants (38 women and 35 men) from an age group of 27.0 ± 5.5 years, who had no history of neurological or psychiatric illness, including substance abuse. At the time of the study, none of the participants was treated with any kind of permanent medication (other than hormonal contraception). The study was performed according to the Code of Ethics of the World Medical Association (Declaration of Helsinki) and approved by the university's ethics committee. All participants gave their written informed consent prior to inclusion in the study.

As data was also acquired for functional studies, further requirements of inclusion were German as native language, absence of hearing impairment, and right-handedness. The latter was assessed with the Edinburgh Inventory [205].

3.2 Data Acquisition

Data acquisition was carried out with a 3 T scanner (Siemens TIM TRIO, Erlangen, Germany). For each participant, a set of structural, T_1-weighted images was acquired with the following specifications: Repetition time TR = 2300 ms; echo time TE = 2.96 ms; inversion time TI = 1100 ms; voxel size: 1 × 1 × 1 mm^3. Diffusion-weighted images were acquired using a Stejskal-Tanner sequence (for details see paragraph *2.1.1 Diffusion Imaging Sequence*, page 19) with TR = 8300 ms; TE = 82 ms; flip angle = 90°; 64 axial slices with a voxel size of 2 × 2 × 2 mm^3. Measurement was carried out along 30 independent directions using a b-value of 1000 smm^{-2}. In order to reduce noise and other statistical artifacts, the

complete data was acquired two times to later average across acquisitions. Additionally, an image with a b-value of 0 s/mm^2 was acquired for coregistration.

3.3 Data Analysis

Preprocessing consisted of segmentation of each participant's respective T_1-weighted structural data, as well as eddy current correction of DTI data. Data analysis comprised selection of seed regions and probabilistic fiber tracking.

3.3.1 Preprocessing of Structural Data and Seed Definition

High-resolution T_1-weighted 3D data was preprocessed with SPM8 (Statistical Parametric Mapping) [17]. Using image segmentation, separate maps of the whole brain for both grey and white matter structures were extracted (see **Figure 1**). As a result, and in accordance with information from histological studies [37, 167, 280], it was possible to determine the borders of the supracommissural BNST to the cerebrospinal fluid of the lateral ventricle (medial and dorsal to BNST), the white matter of the internal capsule (lateral to BNST) and anterior commissure (running through BNST), and to the anterior portion of the thalamus, which is mainly dominated by its fiber content and hence identified as white matter (caudal to BNST). However, the aforementioned direct proximity of the infracommissural BNST to the nucleus accumbens, the basal forebrain, the preoptic area, and the septal nuclei [149], did not allow definition of ventral, ventromedial, rostral, and lateral subcapsular borders of the BNST on the basis of T_1-weighted structural data. In favor of a conservative approach, i.e. to avoid contributions of neighboring structures when defining the seed masks, only voxels in level with, or dorsal and posterior of the anterior commissure were considered.

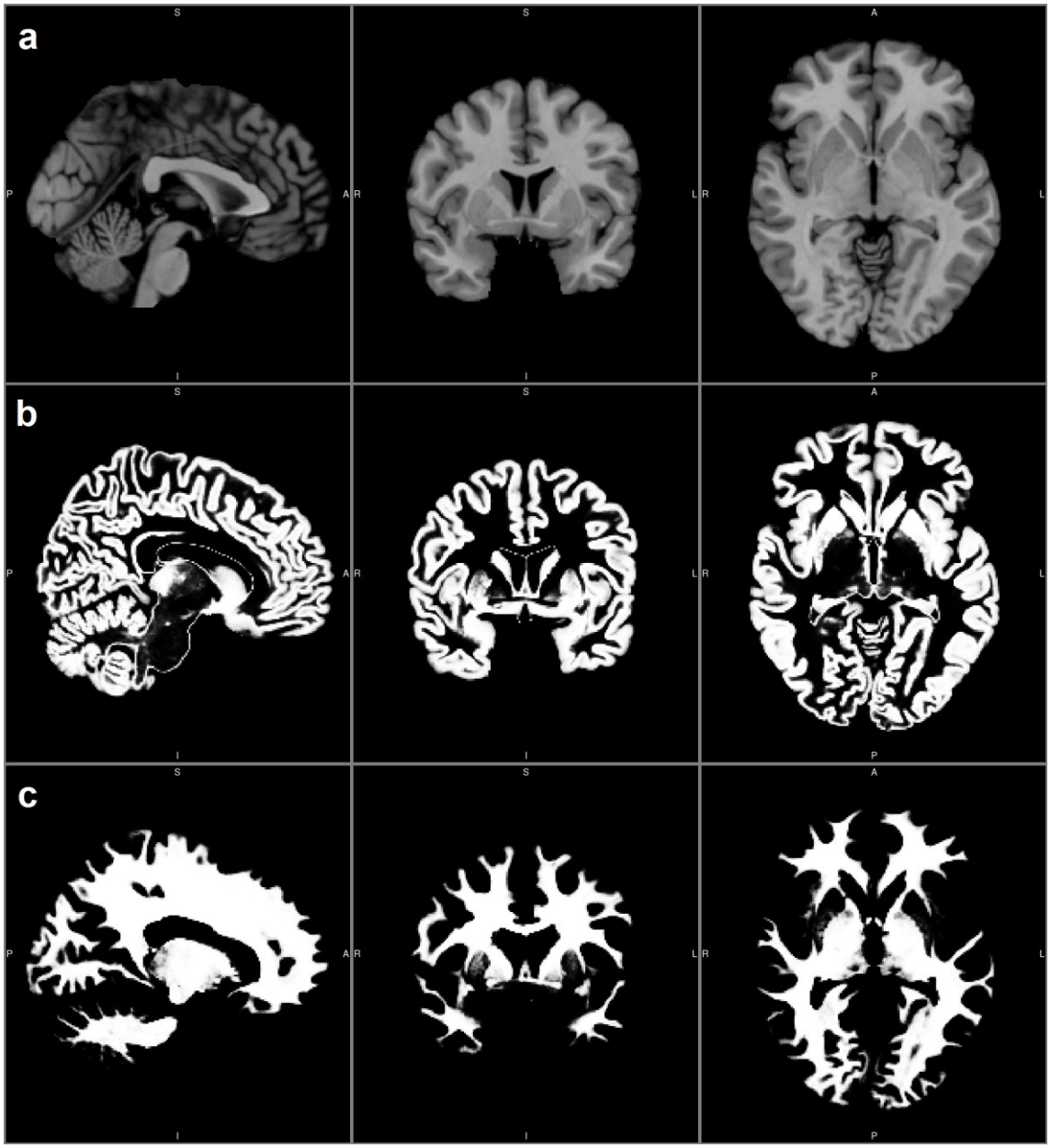

Figure 1 *Image segmentation of (a) high-resolution T_1-weighted anatomical data, in this figure's case the Colin27 MNI standard brain [127], provides binary maps for both (b) gray matter and (c) white matter.*

After determining the coordinates of the seed region, seed masks were cut out of the grey matter maps. This way, inclusion of voxels of adjacent white matter structures, i.e. the anterior commissure, internal capsule, and anterior thalamus, which might evoke false positive results in the fiber tracking process, was prevented. The resulting masks were then converted into binary masks, meaning

that selected voxels of the BNST were ascribed an intensity value of one, while the remaining voxels were zeroed. Finally, they were coregistered to the respective participant's individual DTI data set, with a resampled voxel size of 2 × 2 × 2 mm^3 (i.e. matching the resolution of the diffusion-weighted data).

For means of demonstration (**Figure 2**), individual masks were furthermore transformed to MNI space, added across participants and then projected onto the Colin27 MNI standard brain [127], using FSLView in FSL 4.04 (FMRIB Software Library, Oxford University, www.fmrib.ox.ac.uk/fsl).

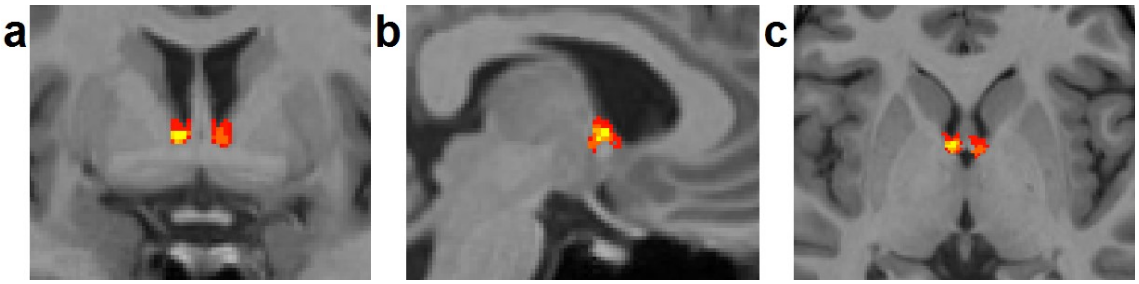

Figure 2 *Individual binary BNST seed masks were transformed into MNI space, added across participants and then projected onto the Colin27 MNI standard brain [127]. Voxels with highest inter-individual overlap are displayed yellow. Coronar (a), sagittal (b) and axial (c) view [155].*

3.3.2 Preprocessing of Diffusion-Weighted Data

Preprocessing and fiber tracking procedures of diffusion-weighted data were performed using FSL 4.04. Eddy current correction, when performed with FSL, is mainly based on two simple assumptions [13]: In the ideal condition of eddy currents not occurring, (1) the diffusion signals of two measurements in exact opposite directions are equal in absolute value, and (2) when acquiring the signal from a voxel in two different diffusion-weighted directions, small angles between these directions produce very similar signals, while larger angles may lead to larger differences between signals. Using these assumptions, a Gaussian process is conducted in order to correct diffusion-weighted data. Subsequently, data was averaged across the two acquisitions, followed by voxel-wise estimation of fiber orientations and uncertainties, as was described in detail in paragraph

2.2.3 Optimizing PFT Methods, page 25 (also see [31, 32]). As a result, maps of the two most probable diffusion directions in each voxel were retrieved.

3.3.3 Probabilistic Fiber Tracking and Depiction of Results

For every participant, the fiber tracking process consisted of four runs, i.e. two for each BNST. Probabilistic fiber tracking was performed with FSL 4.04, starting 5000 times from each voxel of the seed mask. For each BNST seed, fiber tracking comprised one run allowing for a maximum kinking angle of *arccos(0.2)* ≈ 78.5° (FSL standard value), and a second run allowing for a maximum kinking angle of *arccos(0)* = 90°. Detailed information on the probabilistic fiber tracking process has been provided in chapter *2.2 Probabilistic Fiber Tracking*, page 22). After evaluation of the resulting fiber tracks, two further control PFT runs were performed in order to confirm the specificity of the course of the anterior projection (see *4.3 Anterior Projection*, page 37, and *5.2.1 Connections to NAcc and CN*, page 44). One of these runs was conducted starting in a seed region in the head of the CN traversed by the anterior pathway, the other one starting from the immediately adjacent parts of the IC.

PFT was not restricted by (a) waypoint, (b) exclusion, or (c) termination masks. In case (a), only fiber tracks through a predefined waypoint mask would have been displayed in the results; in (b), pathways running through a predefined exclusion mask would have been subtracted from the results; in (c), PFT would have been stopped on the incident of a streamline meeting the termination mask. The resulting fiber track maps were thresholded at 1% of the maximum intensity value so as to reduce false-positive pathways. Individual results for each run were viewed separately and differences between the runs allowing for a kinking angle of 78.5° and 90°, respectively, recorded. These differences will be discussed in chapter *5.4 Methodical Considerations,* page 50.

The thresholded PFT maps of the runs allowing for a kinking angle of 78.5° were then transformed to MNI space, using the specifications gained during the segmentation process. Binary connectivity maps were then created in a way similar to the creation of the binary seed masks. Normalized binary maps were added across participants and voxels common to at least 75% and 90%,

respectively, were displayed using FSLView and 3DSlicer (http://www.slicer.org/, [90]).

3.4 Specimen for Histological Control Experiment

Analysis of PFT results showed, among others, unexpected fiber pathways through the head of the caudate nucleus (for further details see *4.3 Anterior Projection*, page 37, and *5.2 Connections via the Anterior Projection*, page 43). In order to confirm this finding histologically, brain slices were obtained from one specimen of the Tübingen anatomy body donor program. The histological slices shown in this thesis originate from an 88 years old male that was adjudged free from organic brain damage including dementia, cerebral ischemia, and cerebral bleeding. All body donors signed a written consent during lifetime permitting the use of their body and parts for science and teaching. The ethic commission of the University of Tübingen approved the anatomy body donor program and written consent documents with letter 237/2007BO1 [155].

3.5 Microscopic Slides

The anterior midbrain was dissected, and transversal sections of approximately 6mm thickness commencing from the ventral striatum up to the interthalamic adhesion were obtained. The slices were dehydrated and embedded in paraffin wax. The paraffin blocks were cut in slices of approximately 5 µm thickness and mounted on microscope slides. The slides were stained using the silver impregnation technique by Gomori [197].

Images of the microscopic slides were recorded with a digital camera (Zeiss AxioCam MRc, Carl Zeiss Jena AG, Jena, Germany) mounted on a stereo microscope (Leica MZFL III, Leica Microsystems GmbH, Wetzlar, Germany) [155].

4 Results

The following descriptions refer to the results of fiber tracking with a maximum kinking angle of 78.5°. Relevant differences of fiber tracking with a maximum kinking angle of 90° are discussed in chapter *5.4 Methodical Considerations*, page 50, and in *5 Discussion of Study Results*, page 41.

In both hemispheres, fiber tracking of the BNST revealed three distinct projections that run in posterior, ventral, and anterior direction, respectively. Fiber bundles that were consistent in at least 75 % of the study participants are shown as a 3D reconstruction in **Figure 3**.

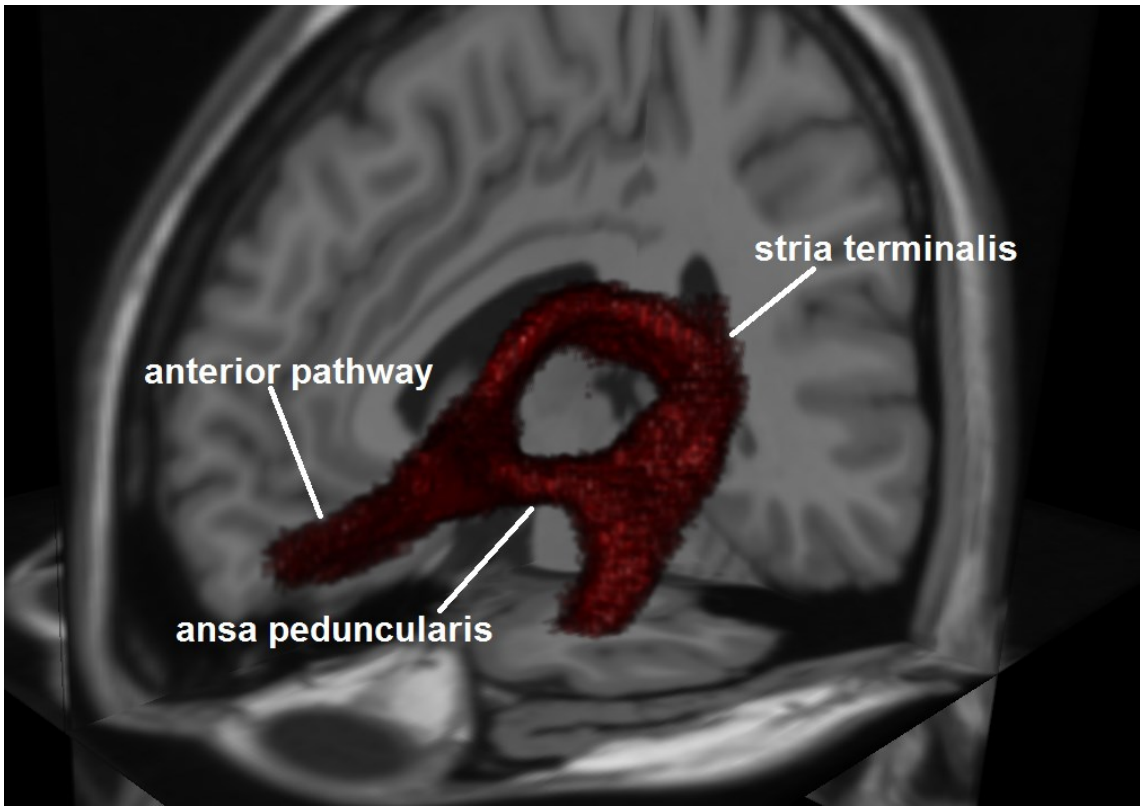

Figure 3 *3D reconstruction of the three main pathways that were tracked from the BNST of the left hemisphere. Displayed are voxels common to at least 75% of the participants. Both stria terminalis and ansa peduncularis reach the amygdala, but from lateral and medial directions, respectively.*

4.1 Posterior Projection

The posterior bundle runs along the ventrolateral margin of the anterior horn of the lateral ventricle, in a hutch between the medial margin of the caudate nucleus and the dorsomedial ventricular surface of the thalamus. It curves around the posterior edge of the thalamus and then continues along the superior margin of the inferior horn of the lateral ventricle, first dorsal and then lateral to the hippocampus. It finally reaches the lateral margin of the amygdala. This finding is consistent with typical anatomical descriptions of the stria terminalis [22, 67, 106, 149] (see **Figure 4**). Branching off this fiber bundle, connectivity results showed voxels indicating structural connectivity towards midline areas of the thalamus, especially in the right hemisphere, as well as to the hippocampi of both hemispheres.

This posterior projection via the stria terminalis towards the amygdala was observed in all participants. In the left hemisphere of 98% of the participants and in the right hemisphere of 97% participants it appeared to continue towards the temporal pole (which was identified using the Harvard-Oxford cortical structural atlas [73]). This finding is in line with recent observations from a study by Avery et al. [21] who were the first to describe a connection of this kind.

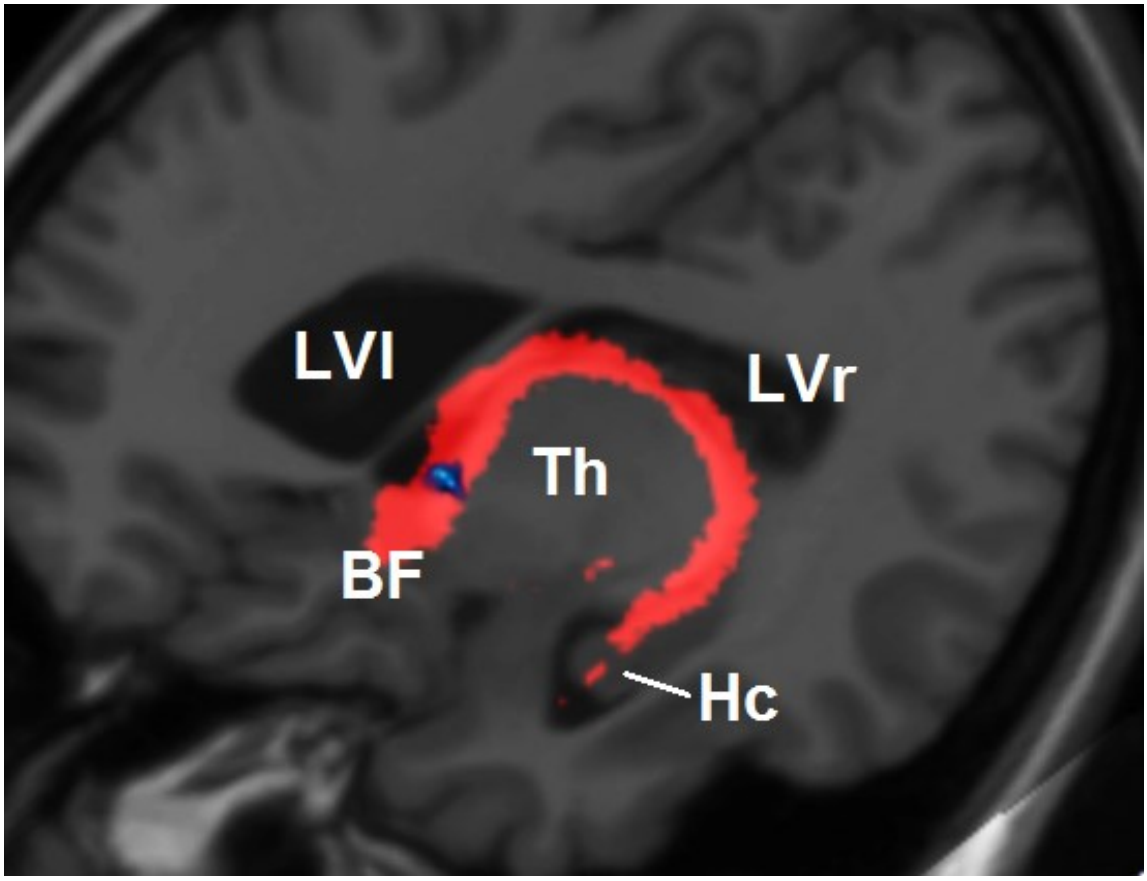

Figure 4 *Oblique reconstruction of the brain sliced in plane with the course of the right stria terminalis (colored red). The location of the BNST seed region is displayed in blue. This figure shows the course of the stria terminalis from the hypothalamic/basal forebrain region (BF) along the ventricular surface of the thalamus (Th) to hippocampal regions (Hc) neighboring the amygdala. Connections to the amygdala and the temporal pole are out of this plane and therefore not pictured. LVl, left lateral ventricle; LVr, right lateral ventricle.*

4.2 Ventral Projection

The ventral bundle descends from the BNST, passing the anterior commissure at its posterior border, into the ventral parts of the basal forebrain. There, it diverges into two separable pathways, of which one terminates in the hypothalamus, while the other turns laterally to reach through the substantia innominata towards the medial and dorsoposterior margin of the amygdala. It furthermore appears to reach farther caudally, to run along the ventral border of

both the putamen and the pallidum, and then terminate in the white matter of the posterior insular cortex (see **Figure 5**). This posterior aspect of the ventral pathway shows remarkable overlap with the posterior limb of the anterior commissure.

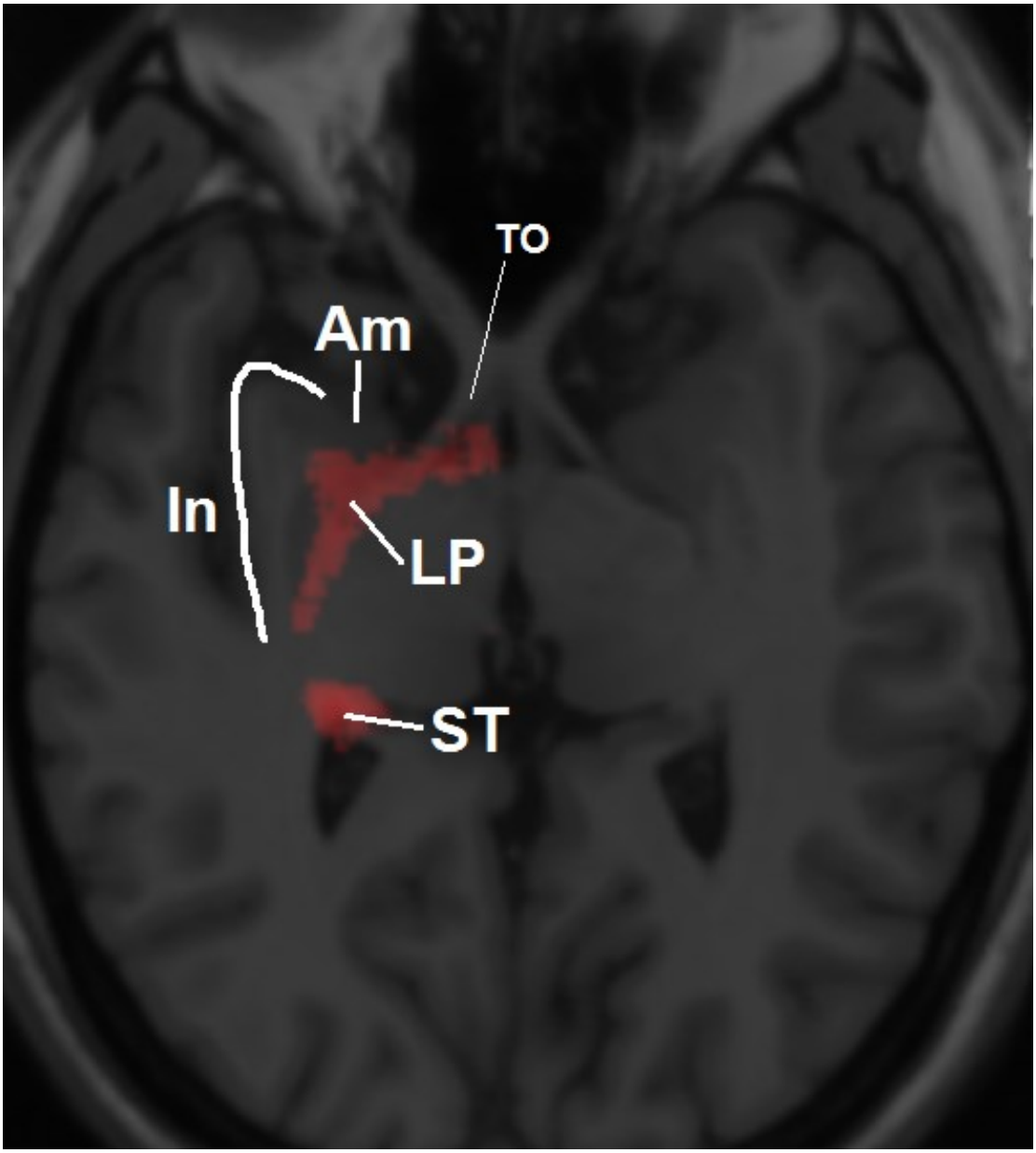

Figure 5 *Reconstruction of the brain sliced slightly oblique in plane with the course of the right lateral pathway (LP). After crossing above the optic tract (TO) it reaches the amygdala (Am) at its posterior margin, and then runs posteriorly towards the inferior insular cortex (In), showing strong overlap with the posterior limb of the anterior commissure. ST, stria terminalis.*

The ventral connection towards the amygdala is consistent with the previously described ansa peduncularis (or ventral amygdalofugal/amygdalopetal tract; see [163, 204, 284]; furthermore see paragraph *1.3.1 The Extended Amygdala*, page 4). Connections to the insular cortex have also been observed [143, 185, 240]; however, their functional relevance still has to be investigated.

4.3 Anterior Projection

The anterior bundle crosses the anterior commissure at its dorsal border and then enters the ventral tip of the head of the caudate nucleus, the dorsal part of the accumbens nucleus and the transition area between these structures. It continues towards the white matter of the frontal lobe and then runs subcortically of the medial prefrontal cortex towards the orbitofrontal pole (see **Figure 6**).

In the left hemisphere of 97%, and in the right hemisphere of 93% of the participants, respectively, the anterior bundle reached the frontal pole (as identified with the Harvard-Oxford cortical structural atlas [73]). In the majority of cases, the anterior bundle almost exclusively targeted the most medially and ventrally located regions of the orbitofrontal cortex. When regarding only voxels common to at least 75% of the participants, these cortical termination areas were almost exclusively identified as medial parts of Brodmann's area (BA) 11 and, in some cases, medioventral parts of BA 10 of the orbitofrontal cortex. This identification was performed using the WFU PickAtlas toolbox [179, 180].

.

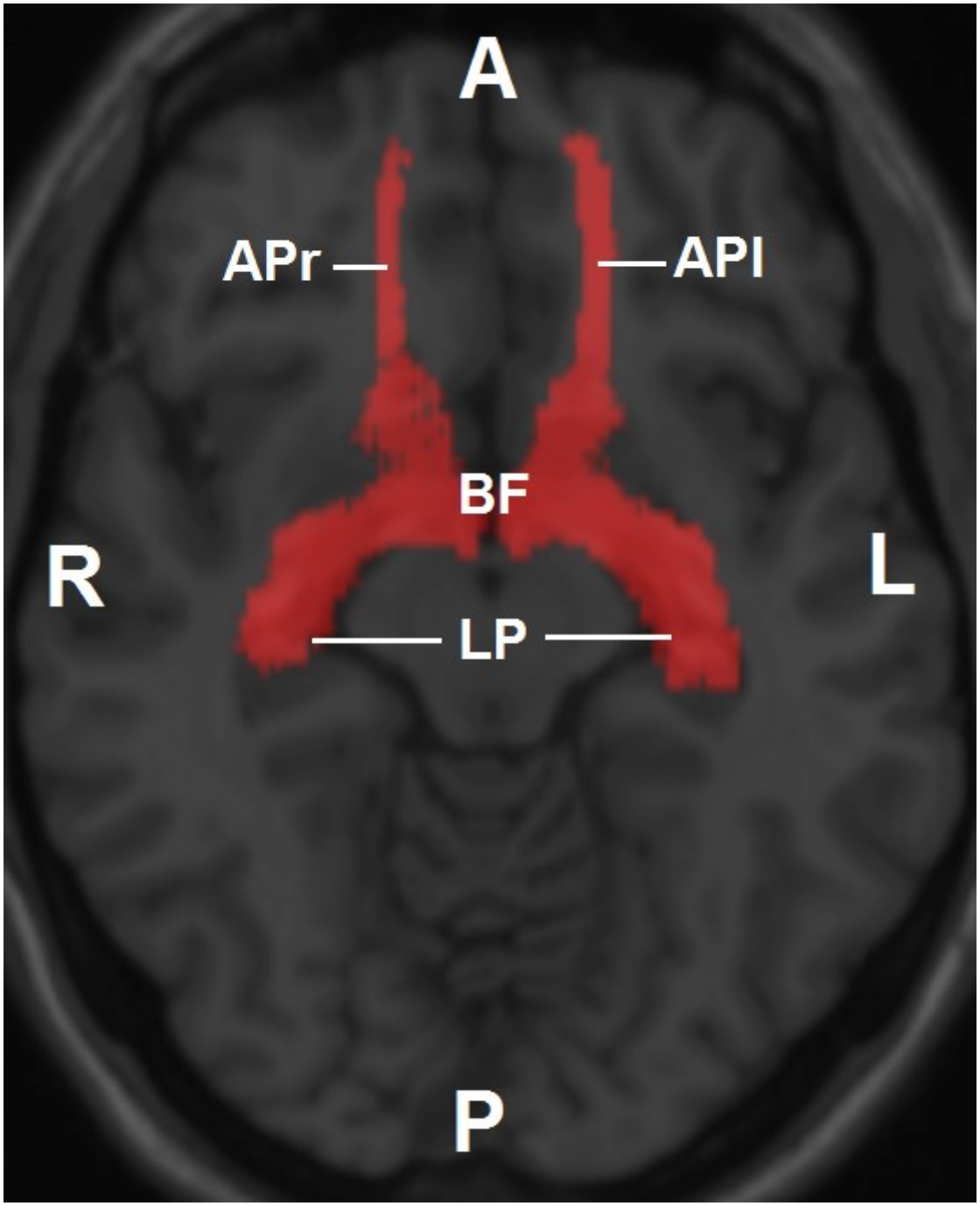

Figure 6 *Axial view of voxels common to at least 75% of the participants in plane with the anterior projection. APl, left anterior projection; APr, right anterior projection; BF, basal forebrain; LP, lateral pathway.*

4.4 Projections towards the Brainstem

Another region repeatedly described to be connected to the BNST and therefore of particular interest in the present study is the brainstem. When performing PFT starting from the left hemisphere's BNST, connections to brainstem structures were observed in 78% of the participants, with 21% terminating in the midbrain and 57% also reaching lower brainstem regions. PFT starting from the right hemisphere's BNST revealed brainstem connections in 81% of the cases, with 7% terminating in the midbrain and 74% reaching lower brainstem regions. However, these connections show great inter-individual variability in their exact course and targets. As a result, no common pathways towards brainstem structures can be observed when looking at voxels common to at least 75% of the participants. Possible problems concerning PFT towards brainstem structures are discussed in chapters *5.3 Irregularity of Connections to the Brainstem*, page 49, and *5.4 Methodical Considerations*, page 50.

4.5 Results from Histological Control Experiment

In order to substantiate the finding that the anterior bundle reaches the white matter of the frontal cortex mostly through the CN and NAcc, histological slices of the head of the CN were stained for neural fibers. It was possible to identify a rostrally oriented fiber bundle of more than 2 millimeters in diameter perpendicularly crossing the anterior commissure and entering the head of the CN (**Figure 7**a,b). These fibers were easily distinguished from the IC since they are located far more medially. Branches of this bundle could then be followed about halfway through the rostrocaudal extent of the head of the CN (**Figure 7**c) until they left the plane of the histological slice and were only partially visible in more ventrally positioned slices due to their oblique course in rostroventral direction (**Figure 7**d). Similarly, in a plane located ventrally to the anterior commissure several parallel fiber bundles with a combined diameter of over 3 millimeters were observed to emerge rostrally from the head of the CN and enter the white matter of the prefrontal cortex where their lateral fibers partly intertwine with medial aspects of the IC (**Figure 7**e) [155].

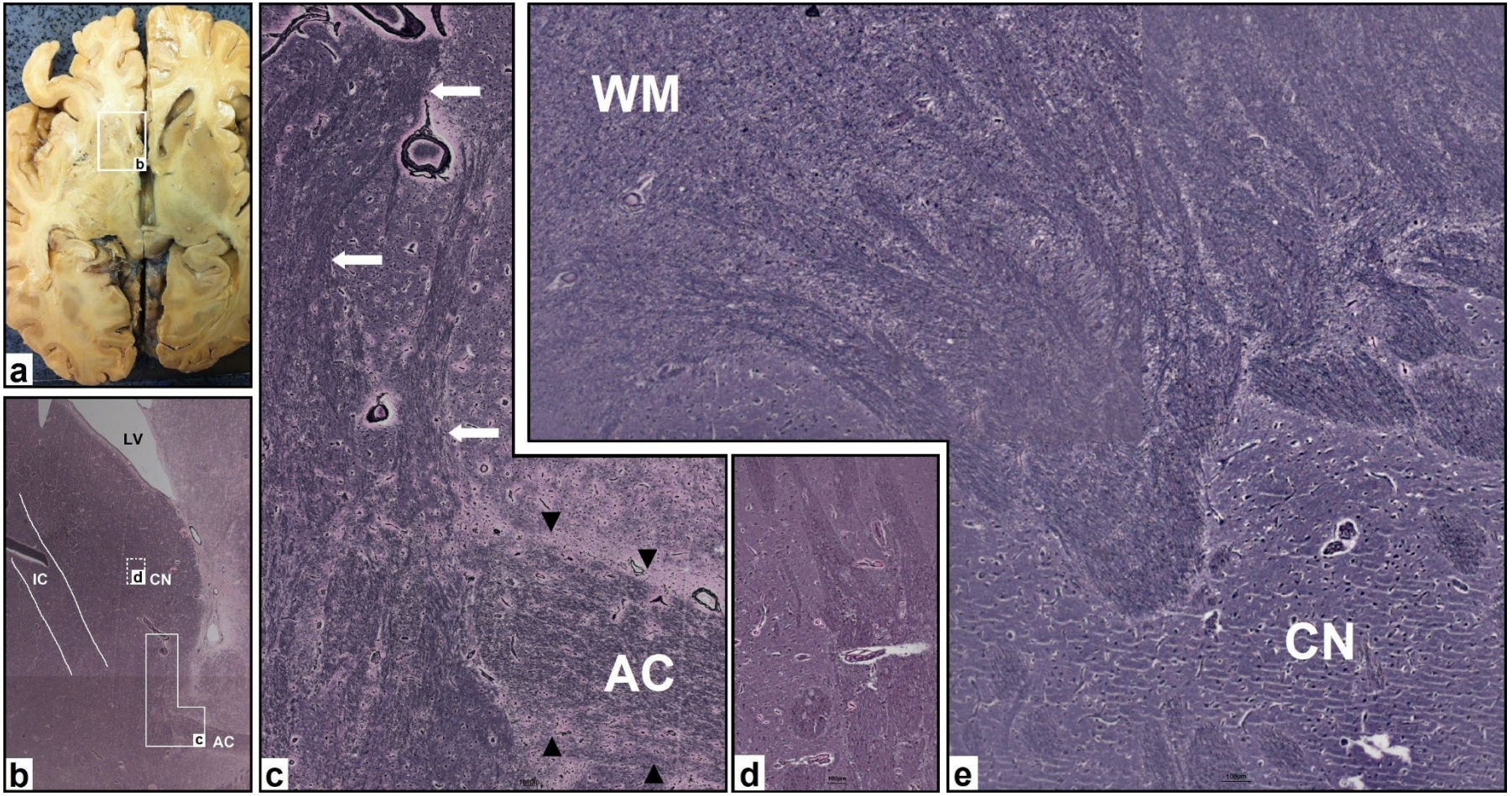

Figure 7 *Histological confirmation of a rostrocaudally oriented fiber pathway through the head of the CN; a) macroscopic overview; b) microscopic overview of the area marked in a) at low magnification; c) detailed view of the area marked in b), where the anterior commissure (AC; indicated by black arrowheads) is crossed by a rostrocaudally oriented fiber bundle (indicated by white arrows); d) representative fibers in the middle of the head of the CN (slice position indicated by dashed lines in b)) as observed in a slice located several µm further ventrally; e) fiber bundles emerging from the head of the CN and entering the white matter (WM) of the prefrontal cortex. IC, internal capsule, LV, lateral ventricle [155].*

5 Discussion of Study Results

The study described in this thesis aimed at delineating the structural connections of the BNST in the human brain in vivo, using probabilistic fiber tracking (PFT) of diffusion-weighted magnetic resonance imaging (DW-MRI) data. The results showed three distinct pathways that occurred consistently across most participants. (1) The posterior bundle curves around the thalamus to reach the lateral margin of the amygdala. This projection matches general descriptions of the stria terminalis [22, 67, 106, 149]. (2) The ventral bundle connects the BNST to adjacent basal forebrain regions and, with its laterally reaching portion, the dorsoposterior margin of the amygdala. It then runs along the ventral boarder of the putamen and pallidum towards the insular cortex. This pathway is consistent with a bundle described as the ansa peduncularis [163, 204, 284], and its posterior part shows strong overlap with the posterior limb of the anterior commissure. (3) Finally, the anterior bundle traverses the junction area of the nucleus accumbens and caudate nucleus, enters the prefrontal white matter and reaches the medial prefrontal cortex (mPFC) and orbitofrontal cortex (OFC). While the posterior and ventral projection perfectly match knowledge obtained in animal studies, arguing for a strong similarity across species, the anterior projection has not yet been described in the extent observed in this study.

It is notable that, although fiber tracking results were not limited by exclusion masks and despite the BNST's close proximity to the anterior commissure, the found projections were strictly limited to their respective hemisphere. This is consistent with previous observations that in the primate brain, only an insignificant amount of stria terminalis fibers crosses to the contralateral hemisphere via the anterior commissure (for a review see [67]).

5.1 Connections via Stria Terminalis and Ventral Pathway

While both stria terminalis and ansa peduncularis mainly interconnect BNST, amygdala and hypothalamus, several further regions that have been reported to be connected to the BNST are probably reached, among others, via one of these

two pathways. Several nuclei of the thalamus (e.g. [81, 170, 240, 274]), as well as parts of the hippocampus, mainly the ventral subiculum [41, 185, 284] and ventral parts of CA1 [79, 198], are probably reached by fibers of the stria terminalis and the ansa peduncularis. However, since both thalamus and hippocampus lie immediately adjacent to the stria terminalis, PFT results can neither confirm nor disprove structural connectivity with certainty. In addition, there have been observations of the thalamus being reached via different pathways, such as the medial forebrain bundle [82] or via fibers directly entering the thalamus at its border to the BNST [81]. Furthermore, Canteras et al. [41] stated that only a few hippocampal afferents reach the BNST through the stria terminalis and ansa peduncularis, while the majority courses through the precommissural component of the fornix.

The ventral pathway found in the present study shows strong overlap not only with the ansa peduncularis, but also with the posterior limb of the anterior commissure. A likely interpretation of this fact would be that fibers related to the BNST either represent a part of the posterior limb of the anterior commissure themselves, or that they are interconnected with cells of the interstitial nucleus of the posterior limb of the anterior commissure (IPAC). As Alheid et al. [5] demonstrated, the ventrolateral BNST and the IPAC blend within the substantia innominata, and a subsequent study showed direct fiber connections between the lateral part of the supracapsular BNST and the IPAC [238]. Furthermore, the BNST has been shown to receive inputs from the insular cortex mainly via the posterior, temporal limb of the anterior commissure [97]. The assumption of a direct anatomical connection between BNST and insular cortex is enforced by observations that both regions are differently involved in substance dependence and drug withdrawal [200, 202, 232], in the development of taste aversion [134, 223], and in regulation of cardiovascular function [292], especially in response to stress [44, 58].

The PFT results furthermore arouse the suspicion that the ventral pathway also contains connections towards the putamen and pallidum. Several authors have described BNST connectivity, both anatomically [80, 81, 113], as well as functionally [235], with parts of the basal ganglia, foremost the nucleus

accumbens and the ventral striatopallidum (i.e. the transition zone of nucleus accumbens and caudate nucleus). However, specific connections of the BNST to the putamen and globus pallidus, to the author's knowledge, have not been described yet. Haber et al. [112] reported enkephalin-immunoreactive ramifications throughout the globus pallidus with single fibers reaching the ventral striatum, the amygdala, the BNST and hypothalamic regions, respectively, but the functional significance of those fibers entering the BNST remains unclear.

It has to be considered that the observed fibers towards more caudally located parts of the ventral putamen and pallidum are closely related to the ansa peduncularis, but do not originate in the BNST but rather in the amygdala. This assumption is in line with observations by Fox [96] who, in a study on the cat brain, reported fibers similar to those connecting amygdala and preoptic area (i.e. the ansa peduncularis) running from the amygdala to the nucleus entopeduncularis (which is equivalent to the medial segment of the globus pallidus in primates). Furthermore, Russell et al. [225] reported evoked responses in the putamen as a result of electrical stimulation of the amygdala in cats. Only recently, an fMRI study in humans revealed a correlation between trait extraversion and resting state functional connectivity of the amygdala and, amongst others, the putamen [2], which might point towards heightened reward sensitivity. However, the BNST itself appears not to contribute to this amygdalostriatal projection [145].

5.2 Connections via the Anterior Projection

The anterior projection courses through the nucleus accumbens (NAcc) and the head of the caudate nucleus (CN), enters the white matter of the prefrontal cortex and reaches the orbitofrontal cortex. While some of its aspects match knowledge obtained from animal studies, others have not been observed to this date and therefore have to be discussed in regard to functional and methodical (see *5.4 Methodical Considerations*, page 50) considerations.

5.2.1 Connections to NAcc and CN

One interesting aspect of this connection is the fact that it appears to run straight through the rostroventral tip of the CN and the adjacent transition zone to the NAcc. BNST and stria terminalis projections to and from the nucleus accumbens have previously been described [65, 77, 79, 80, 113, 149]. They are in line with a variety of study results linking both structures to mutual tasks. While the BNST has major impact on the expression of anxiety and has been linked to depression (see chapters *1.5.1* and *1.5.2*), deep brain stimulation of the NAcc in a mouse model of enhanced depression- and anxiety-like behavior has been reported to elicit anxiolytic and anti-depressive effects [236]. NAcc activity has been shown to display complex changes during anxiety-related avoidance [169], and results from a study by Radke et al. [217] suggest that anxiety during drug withdrawal, in which the BNST plays a major role (see paragraph *1.6.1 The BNST's Relevance to Substance Dependence*, page 14), might follow from a decrease in dopamine levels in the NAcc. Finally, cues predicting reward lead to increases of dopamine levels in both NAcc and parts of the BNST [211] (also see paragraph *1.6.1 The BNST's Relevance to Substance Dependence*, page 14, for the BNST's role in communicating rewarding effects of substance consumption).

Surprisingly, the results of the study at hand also revealed fibers passing through the ventral tip of the head of the caudate nucleus (see **Figure 8**). A pathway from the BNST or ST running to or through the CN has not been reported yet. However, strong evidence for a rostrocaudally oriented bundle through the ventralmost part of the head of the CN and to the mPFC could be seen on histological preparations of the head of the CN from human brains, as described in chapter *4.5 Results from Histological Control Experiment*, page 39.

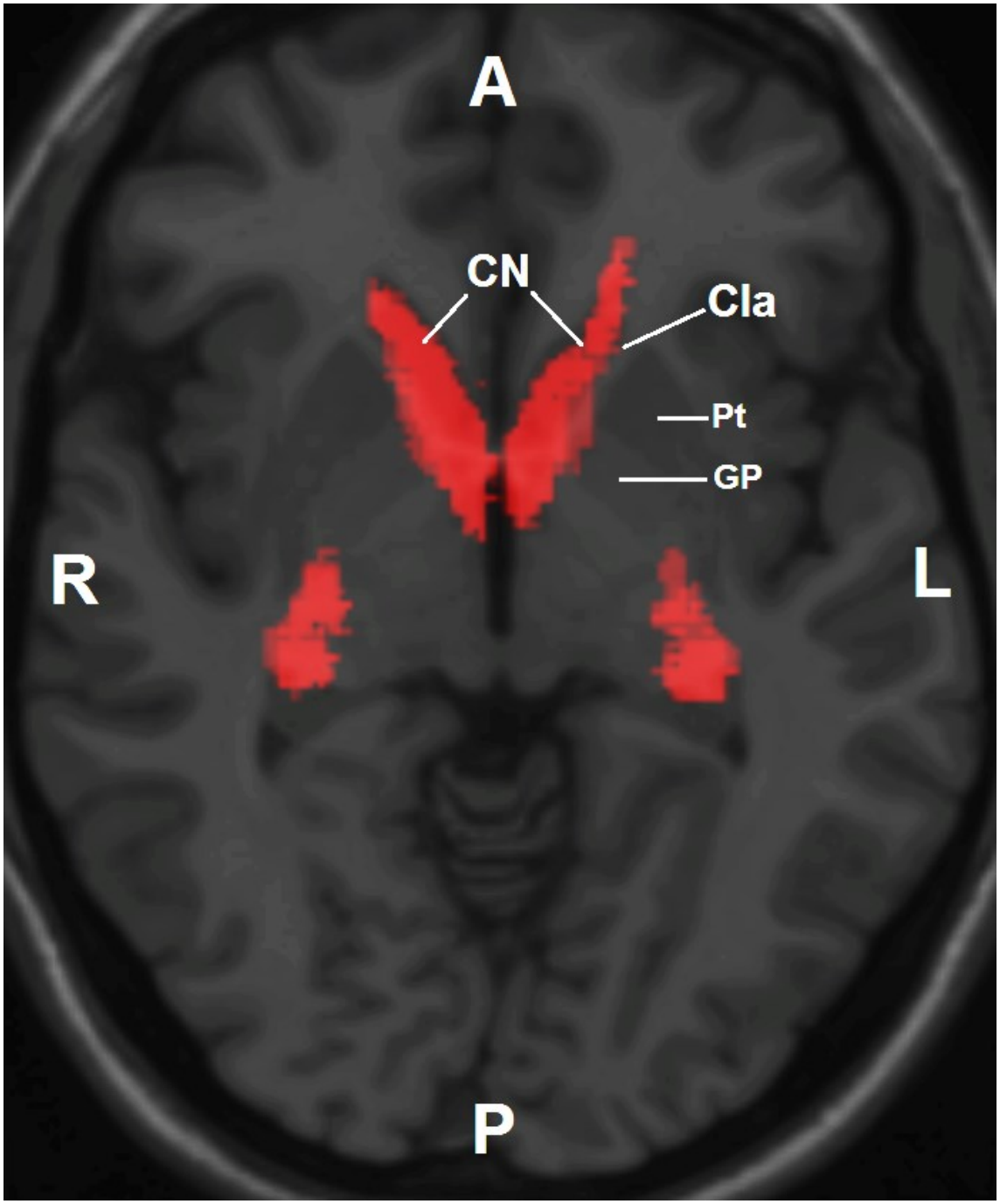

Figure 8 *Trans-caudate portions of the anterior projections when displaying voxels common to at least 75% of participants. In order to reach the white matter of the medial prefrontal cortex, the anterior pathway traverses the head of the caudate nucleus (CN) rather than travelling through the crus anterior of the internal capsule (Cla). GP, globus pallidus; Pt, putamen.*

These findings are furthermore well in line with DW-MRI results published by Kotz et al. [152], who examined the internal and external connectivity structure of the CN. Accordingly, on the individual participants' maps of the most probable diffusion direction in the data acquired for this study, the main eigenvectors of the diffusion tensors in those voxels of the head of the CN that the anterior pathway passes through are oriented parallel to the course of the anterior pathway (see **Figure 9**). In addition, FA in those voxels in almost all cases ranges above 0.2, in some cases reaching values of up to 0.5, indicating that the directionality of diffusion in this area is considerably more pronounced than in cortical grey matter structures [176].

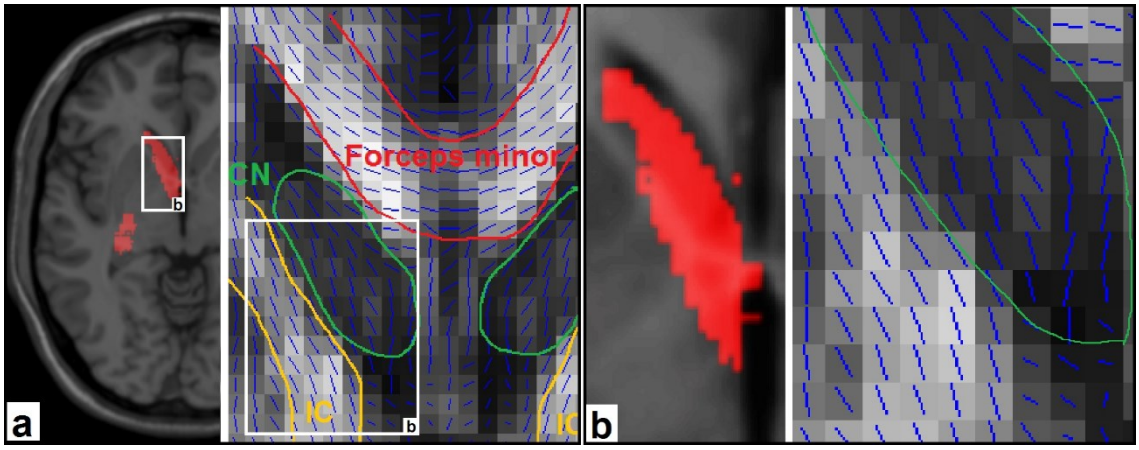

Figure 9 *MRI images of the trans-caudate portion of the anterior pathway; a) overview, b) detailed view of the respective area marked in a). The left images show voxels from fiber tracking results (red) common to at least 90% of participants. The blue lines in the right images show the direction of the diffusion tensor's principal eigenvector of each voxel in the brain of one representative participant. They indicate that the main direction of diffusion throughout most of the head of the caudate nucleus is almost parallel to the main direction of diffusion in the internal capsule. CN, caudate nucleus, IC, internal capsule [155].*

Finally, control PFT runs starting in those parts of the head of the CN that are traversed by the anterior pathway in all participants revealed a significant number of fiber tracts running to the BNST and into the ST, as well as the ventral pathway, arguing for a neural connection of BNST and CN.

The role of this connection remains unclear, since a functional relationship between CN and BNST is not yet known to exist. Still, these findings indicate that the ventralmost part of the head of the CN, much like the NAcc and the ventral striatopallidum, is also one of the parts of the basal ganglia associated with the limbic system, and not, or at least not only, with the motor system.

It might be argued that the anterior projection shows great resemblance to pathways within the internal capsule and therefore might result from poor coregistration between anatomical and diffusion data. However, there are several points arguing against this objection. For one thing, a pathway through the head of the CN was observed in the majority of participants, which would mean that this finding is due to a systematic error in the coregistration process. Since coregistration was automatically performed with SPM, an error like this would very likely have been discovered in earlier studies using the same software. Moreover, projecting the PFT results directly onto a diffusion-weighted volume, which still allows clear differentiation between CN and internal capsule, confirms that the anterior pathway travels through the CN and not the anterior limb of the internal capsule. Lastly, a direct comparison of the abovementioned PFT results starting from a CN seed with PFT results starting from a seed of the immediately adjacent internal capsule revealed that, while the CN shows strong connectivity overlap with the BNST, the anterior limb of the internal capsule reveals almost no structural connectivity with the BNST, the ST and the ventral pathway.

5.2.2 Connections to mPFC and OFC

Several animal studies have provided evidence for connections between the BNST and caudal parts of the medial prefrontal cortex (mPFC), e.g. in the rat brain mainly the infralimbic area (IL, area 25) [79, 81, 240, 273] and, however to a much lesser extent, the prelimbic area (PL, area 32) [185]. For that matter, the BNST is assumed to be an important relay for interactions of the mPFC and the paraventricular nucleus of the hypothalamus (PVH) [248]. Furthermore, the BNST as a relay structure is a likely candidate for mediating functional

disconnection of mPFC and amygdala observed as a result of drug withdrawal in animals [101].

The results of the study at hand show fiber tracts that reach farther rostrally. They pass by BA 25, a likely primate equivalent to the rodent's IL [268], as well as the most inferior parts of BA 32, a likely primate equivalent to the rodents PL [268], and connect the BNST and OFC, an observation that, to the author's knowledge, has not yet been made. These structural findings are, however, in line with functional activation data reported by Fox et al. [95] suggesting a close functional interplay between OFC and BNST in non-human primates. More precisely, Fox and colleagues reported a decrease in both BNST metabolism and freezing behavior in OFC-lesioned animals compared to controls. Concordantly, recent results by Motzkin et al. [196] indicate functional connectivity between BNST and OFC in healthy humans as well as decreased blood flow in the right BNST during rest in neurosurgical patients with lesions to the OFC which, in all examined patients, contained the areas targeted by the anterior pathway. While neither amygdala nor CN showed altered blood flow during resting state as a result of these OFC lesions, functional coupling of OFC and amygdala in processes that are likely to further involve the BNST (such as threat-induced anxiety) has been reported both in non-human primates [226] and in humans [105]. Moreover, mPFC-lesioned animals have been shown to express increased PVH activity in response to stressors, an effect that is possibly mediated by the BNST as well [248]. These findings point towards a role for these structures, as well as their connections, in the regulation of behavior in a threatening context, which might therefore be of relevance in anxiety disorders in humans. In line with this hypothesis, patients with social anxiety disorder (SAD) were found to exhibit increased amygdalar activity during emotional face perception [114] in addition to a disrupted connectivity of the amygdala with the OFC [245]. While recent structural connectivity data revealed reduced volumes in fiber projections between the anterior temporal lobe and the OFC via the uncinate fascicule [27], connections involving the BNST and its projections have not been examined yet. Boehme et al. [36] explicitly reported that they observed no significant differences in BNST activity in SAD patients compared to healthy controls in a context of

predictable external stress signals. BNST activity in SAD patients during anticipation of unpredictable threat to this date remains unexamined; still, Lee et al. [161] reported an increase in anxiety-like behavior in rats during social interaction as a consequence to intra-BNST injection of CRF agonists in doses below the threshold for inducing acute changes in an exploratory task. These findings indicate an involvement of the BNST in the expression of social anxiety in a way that the BNST elevates social anxiety as a result of chronic stress. Since prefrontal cortex regions have been shown to suppress HPA activity, with the BNST as a possible relay (as described in paragraph *1.5.3 The BNST's Influence on Autonomic Reactions to Stress*, page 10), and disrupted connectivity of OFC and amygdala has been shown in SAD patients [245], it appears highly likely that the BNST is part of this neural circuitry responsible for the expression of social anxiety.

It has to be taken into consideration that the observed frontal projections are not related to the BNST, but instead represent pathways between prefrontal areas and other brain regions, especially the amygdala. Several examinations have reported such connections; Kelley et al. [145] described amygdalostriatal projections in the rat that run both via the longitudinal association bundle and the stria terminalis and that widely overlap striatal connections to the mPFC, while not involving neurons in the BNST; Canteras et al. [40, 42] later showed direct connections between amygdala and mPFC via the stria terminalis in rats. Meanwhile, in a study in monkeys, Leichnetz et al. [165] stated that the majority of amygdala-to-mPFC connections use a pathway that does not include the stria terminalis or its bed nucleus. More recently, DTI experiments reported only non-strial pathways between amygdala and mPFC in humans [20, 147].

5.3 Irregularity of Connections to the Brainstem

Unexpectedly, BNST connections to the brainstem were only observed when looking at the participants' individual results, but with great inter-individual differences in exact course and target areas. So far, pathways connecting the BNST and the brainstem have been described repeatedly in various animals (e.g.

[77, 79-81, 108, 128, 191, 220]), where they are thought, among other things, to mediate the BNST's influence on cardiovascular function [59, 116]. Furthermore, these connections have been implicated in the context of rewarding versus aversive motivation [138] which are subserved by mainly monoaminergic projections [240] that modulate the BNST's influence on hypothalamo-pituitary-adrenal axis (HPA) activity and withdrawal-related behavior [19, 71, 89, 166]. It seems likely that similar functional relationships between the BNST and the respective brainstem regions exist in humans, and therefore that their structural connections are mostly homogeneous as well.

An explanation to be considered might be that the starting region for fiber tracking was limited to supracommissural parts of the BNST. In this case, the observed connections could be a result of random fiber tracking of pathways towards the brainstem originating from other brain structures. It should be noted, however, that several authors specifically described anatomical connections between the dorsal BNST and brainstem in animals [3, 77, 80, 81, 108, 191, 220]. It therefore appears more likely that the results at hand are possibly due to technical limitations of DW-MRI data processing, as will be discussed below.

5.4 Methodical Considerations

One limitation of the study at hand concerns the internal anatomy of the BNST. Various studies have suggested that there are distinct subsections of the BNST with connections to different parts of the amygdala and other brain regions [77, 79-81, 284]. As delineation of the BNST relied on segmentation of T_1-weighted images, it was not possible to separate the infracommissural parts of the BNST from surrounding grey matter structures, such as the preoptic area and substantia innominata, which can only be distinguished by histological techniques [37, 167, 280]. In favor of a conservative approach, the seed area for fiber tracking was therefore restricted to the supracommissural part of the BNST, which features explicit borders in MRI.

As delineated in *2 Diffusion Weighted Imaging and Probabilistic Fiber Tracking*, pages 19 through 26, probabilistic fiber tracking is based on complex statistical

networks that require automatic relevance determination [177] in order to achieve reliable results with acceptable performance. With the given b-values and gradient pulse durations used for data acquisition in the present study, the Bayesian estimation analysis approach in the model proposed by Behrens et al. [32] in most cases provides a maximum of two relevant fiber directions per voxel. As both the stria terminalis and the ventral pathway are quite strong bundles, this possibly might account for missing further, smaller fiber tracts as, for example, connections to the brainstem. Moreover, the maximum angle at which a fiber may kink (regarding the angle between the entry and exit direction within a voxel) has to be restricted in order to avoid false-positive results or redundancy. The algorithm implemented in FSL [32] allows wide angles compared to other approaches; in the present study, kinking of up to 80°, approximately, was tolerated. In some cases, however, the restriction of the maximum angle might result in false-negative results, especially if a small bundle branches off a stronger one at a wide angle. Increasing the maximum angle to 90° yielded connections to lower brainstem regions in further participants, but those now unselectively involved most of the brainstem and even the cerebellum, and they showed even more inter-individual variability, thus indicating that increasing the angle beyond 80° dramatically diminishes the specificity of the probabilistic fiber tracking approach. These findings suggest that the implemented restriction represents one of the major reasons for the lack of common projections towards the brainstem.

It has been suggested that the BNST receives afferents from, and sends efferents to the amygdala, both through the stria terminalis (for a review see [284] as well as the ventral pathway [204], and many regions of the basal forebrain have been shown to share bidirectional connections with the BNST (e.g. [61]). Connections to the insular cortex have been reported to be almost exclusively unidirectional, with the insula projecting towards the BNST [219, 230]. Research on connections between mPFC and BNST has mainly focused on mPFC efferents (e.g. [47, 248, 260]), while, to the author's knowledge, BNST inputs to the mPFC have not been described yet. However, DW-MRI only allows identification of the axis along which diffusion is most likely, but not of the direction in which information (in the

form of action potentials) is mainly passed. Furthermore, it is not possible to display synapses, and therefore it is neither possible to determine if a connection is mono- or oligosynaptic, nor in how far fibers running through the BNST are interconnected with its neurons or only passing through.

As the diameter of axons is much smaller than the voxel size of the diffusion-weighted data, it is furthermore possible that inputs to a brain structure from two different regions appear as a continuous bundle, while they might not even converge onto the same neurons in this structure. This might be of relevance for the observed connections between BNST and OFC, since BNST or amygdala connections to the ventral striatum might overlap with fiber tracts between ventral striatum and OFC [145, 162].

5.5 Conclusion and Perspective

In the current study, the structural connectivity profile of the human BNST was delineated on the basis of DW-MRI. Several connections were identified in line with histological results from animal studies, i.e. the stria terminalis as a posterior pathway to the lateral amygdala, and a ventral pathway towards the hypothalamus as well as the medial amygdala via the ansa peduncularis, which then joins the posterior limb of the anterior commissure to reach the insular cortex. These connections have already been described in animal models, arguing for a strong preservation of these connections across species.

Connections with brainstem areas were found in only a few participants, and with great inter-individual variability, which is probably due to methodological limitations of DW-MRI.

Interestingly, the data at hand indicates the existence of a fiber connection between the BNST and the frontal pole of the OFC. While rodent studies failed to identify this connection, recent neuroimaging experiments in macaques indicate a tight functional coupling of these areas which might be specific to primates. Furthermore, the results indicate a possible connection between the BNST and the temporal pole via the stria terminalis, especially in the left hemisphere. This

connection has only recently been described for the first time in humans [21], and its relevance has yet to be investigated.

Despite its limitations, DW-MRI-based PFT proves to be a powerful tool for investigating structural connectivity profiles in the brains of living humans. The results at hand demonstrate both its advantages and drawbacks. Even when performing PFT starting from a seed region like the BNST, which is only a few voxels in size, and surrounded by some of the densest white matter structures of the brain (i.e. the internal capsule and the anterior commissure), the results turn out to be highly reproducible and uninfluenced by these particular white matter tracts. However, they lack a certain degree of detail, which may lead to both false-negative and false-positive results. Nevertheless, comparison of results to anatomical and especially functional knowledge from animals and humans reveals possible new paths towards the understanding of the structural frameworks underlying various functional brain systems.

These new findings on the anatomical connectivity profile of the BNST pave the way for future research on the functional interplay with its connected areas. A main goal for future research may be the investigation of aberrations of this profile in a variety of psychiatric illnesses, foremost in anxiety and substance abuse. Moreover, divergence between different groups of individuals, for example with regard to personality features, might aid in identifying persons at risk for typical BNST-associated disorders.

III Summary

The bed nucleus of the stria terminalis (BNST) is a heterogeneous basal forebrain structure that surrounds the anterior commissure near its decussation. Its ventral portion is intercalated with other basal forebrain structures such as the substantia innominata, the preoptic area, the interstitial nucleus of the posterior limb of the anterior commissure, and parts of the hypothalamus, with single cell clusters reaching as far as the medial border of the amygdala.
The BNST is functionally related to the limbic system and represents a part of the extended amygdala. It is strongly involved in maintaining an anxious state in the presence of mainly sustained, contextual threats. It integrates inputs from both cortical (e.g. medial prefrontal and insular cortices) and brainstem (e.g. ventral tegmental area, nucleus of the solitary tract) regions and mediates hormonal reactions to stress, mainly by influencing the paraventricular nucleus of the hypothalamus, the main impulse generator for the hypothalamo-pituitary-adrenal hormone axis. In addition, the BNST acutely affects other stress-processing networks (e.g. the parabrachial nucleus), thus exerting influence on cardiovascular function.
The BNST is also involved in a number of pathological processes. It is believed to be crucial for the experience of affective components of drug withdrawal and therefore for the upkeep of substance dependence and drug-seeking behavior. It furthermore has been discussed to be related to phobias and anxiety disorders, as well as eating disorders. Finally, its affection in neurodegenerative diseases might contribute to the clinical symptoms of these illnesses.

Diffusion-weighted magnetic resonance imaging is based on the principle that diffusion in nerve fibers is barely limited in an axial direction, while perpendicular diffusion is restricted by cell membranes and glial cells. Applying diffusion gradients in multiple directions allows reconstruction of a diffusion tensor that describes strength and directionality of diffusion in the respective voxel. Probabilistic fiber tracking (PFT), using a Bayesian model for probability density

functions, then allows estimation of diffusion streamlines that, when performed multiple times and added up, provide reliable estimates of anatomical fiber courses.

In the experiment described in this thesis, the BNST was identified on T_1-weighted anatomical images, and masks of the dorsal BNST, which, other than its ventral parts, provides clear borders, were created and used as seed masks for PFT. PFT was performed on the diffusion-weighted data of 73 healthy participants and fiber tracts common to the majority of these participants were analyzed and discussed in regard to knowledge derived from animal studies.
Three main pathways were observed: (1) A posterior pathway was identified as the stria terminalis. (2) A ventral pathway was seen to connect the BNST to other basal forebrain structures and to the amygdala, consistent with previous descriptions of the ansa peduncularis. It furthermore showed strong overlap with the posterior limb of the anterior commissure, connecting the BNST with inferior parts of the insular cortex. (3) An anterior pathway was observed to traverse both nucleus accumbens and the ventral tip of the head of the caudate nucleus (CN), enter the white matter of the medial prefrontal cortex and reach the pole of the orbitofrontal cortex (OFC).
Connections of the BNST to the CN have not been described yet but are in line with descriptions of the internal connectivity profile of the CN. They possibly indicate an involvement of the CN in limbic tasks.
Structural connections of BNST and OFC are not known from animals but are in line with studies indicating functional connectivity between these structures in monkeys and humans. Their integrity might play a role in anxiety disorders.
BNST connections to the brainstem could only be observed with great inter-individual variability. Since such connections have been described in various animals, this result can likely be ascribed to limitations of PFT. When increasing the maximum angle for fiber kinking while performing PFT, such connections were seen more regularly, but showed great inter-individual variation, indicating considerable loss of specificity.

Zusammenfassung in deutscher Sprache

Der Bed Nucleus der Stria Terminalis (BNST) ist ein Kerngebiet des basalen Vorderhirns, das sich durch eine heterogene Histo- und Chemoarchitektur auszeichnet. Er umgibt die anteriore Kommissur nahe ihrer Hemisphärenkreuzung. Während sich sein dorsal der anterioren Kommissur gelegener Anteil deutlich von angrenzenden Strukturen differenzieren lässt, bilden seine ventralen, subkommissuralen Anteile ein Kontinuum mit weiteren Strukturen des basalen Vorderhirns, z.B. mit der Substantia innominata, der Area praeoptica, dem Nucleus interstitialis des posterioren Anteils der anterioren Kommissur, sowie mit Teilen des Hypothalamus. Einzelne Zellverbände des BNST reichen bis an die mediale Grenze der Amygdala im medialen Temporallappen heran.

Der BNST wird funktionell der erweiterten Amygdala als Bestandteil des limbischen Systems zugeordnet. Er spielt eine herausragende Rolle in der Aufrechterhaltung ängstlich-vermeidenden Verhaltens in Gegenwart andauernder, kontextueller Bedrohungen. Er erhält und verarbeitet Information sowohl aus kortikalen Zentren (z.B. aus medialem präfrontalem Kortex und Inselrinde), wie auch aus Zentren des Hirnstamms (z.B. aus der Area tegmentalis ventralis und dem Nucleus tractus solitarii). Unter Berücksichtigung dieser Information reguliert er hormonelle Stressreaktionen, indem er Einfluss auf den Nucleus paraventricularis hypothalami (PVH) nimmt, welcher als zentraler Impulsgeber der Hypothalamus-Hypophysen-Nebennierenrinden-Achse fungiert. Des Weiteren hat der BNST akuten Einfluss auf vegetative Hirnstammzentren (wie beispielsweise den Nucleus parabrachialis) und damit auf stressassoziierte Herz-Kreislauf-Reaktionen.

Der BNST ist zudem in einer Reihe pathologischer Vorgänge involviert. Ihm wird eine Funktion bei der Vermittlung affektiver aversiver Zustände als Folge von Drogenentzug zugeschrieben, womit er zur Aufrechterhaltung von Substanzkonsum und zum aktiven Suchverhalten beiträgt. Darüber hinaus wird eine Beteiligung an Angststörungen und Phobien sowie an Essstörungen diskutiert. Im Zusammenhang mit neurodegenerativen Erkrankungen (z.B.

Alzheimer-Demenz, Chorea Huntington) könnten krankheitstypische strukturelle Veränderungen im BNST zur Ausprägung des typischen klinischen Bildes der jeweiligen Krankheit beitragen.

Diffusionsgewichtete magnetresonanztomographische Bildgebung (DW-MRI) ist ein Verfahren, welches auf der Annahme beruht, dass in Nervengeweben die Diffusion von Wasser in Richtung der Nervenfaser nur geringfügig eingeschränkt ist, während Diffusion senkrecht zur Faserverlaufsrichtung stark durch Zellmembranen und Gliazellen behindert wird. Im Rahmen der Datenerhebung wird die Diffusionsfähigkeit von Wasser in verschiedenen Richtungen durch mehrere Messungen mit unabhängig orientierten Diffusionsgradientenrichtungen ermittelt. Aus den Ergebnissen lässt sich für jeden Bildvoxel ein Diffusionstensor ermitteln, welcher Informationen über Vorzugsrichtungen und Ausprägung der Diffusibilität von Wasser im entsprechenden Voxel enthält. Das Verfahren des probabilistischen Fiber-Trackings (PFT) führt die Diffusionstensoren des gesamten Gehirns einem Bayesschen Netz zu, dessen Lösungen Wahrscheinlichkeitsdichteverteilungen für die Hauptdiffusionsrichtungen der jeweiligen Voxel darstellen. Durch sukzessive Verknüpfung der Information benachbarter Voxel, d.h. durch Fortschreiten von einem Voxel zum nächsten Voxel, der in der geschätzt wahrscheinlichsten Diffusionsrichtung lokalisiert ist, lassen sich nun sogenannte „diffusion streamlines“ ermitteln. Addiert man die Streamlines mehrerer tausend Fibertrackingvorgänge aus einem Startgebiet (der sogenannten „seed region“), erhält man eine zuverlässige Abschätzung der Verläufe von Fasern, die diesen Seed durchlaufen.

Im beschriebenen Experiment wurde zunächst der BNST auf T_1-gewichteten anatomischen Aufnahmen identifiziert. Da der subkommissural gelegene BNST auf diesen Daten nicht von umgebenden Strukturen abgrenzbar ist, wurden Masken der suprakommissural gelegenen BNST-Anteile erstellt, die als Seed für ein PFT dienten. Dieses wurde an den DW-MRI-Daten von 73 gesunden Probanden durchgeführt und die Ergebnisse, die bei der Mehrheit dieser Probanden beobachtet werden konnten, wurden analysiert.

Im PFT zeigten sich drei Hauptpfade als wesentliches Ergebnis: (1) Ein posteriorer Pfad wurde als Stria terminalis identifiziert; er verläuft, vom BNST ausgehend, entlang der ventrikulären Grenze des Thalamus zunächst im Vorderhorn, dann im Unterhorn des lateralen Ventrikels und erreicht den Hippocampus und die Amygdala. (2) Ein ventraler Pfad verbindet den BNST mit weiteren Strukturen des basalen Vorderhirns sowie in lateraler Richtung mit der Amygdala, übereinstimmend mit früheren Beschreibungen der Ansa peduncularis. Er nimmt dann einen nach posterolateral gerichteten Verlauf, wobei deutliche Übereinstimmung mit dem Verlauf des posterioren Anteils der anterioren Kommissur zu erkennen ist, und endet im inferioren Anteil der Insula. (3) Ein anteriorer Pfad durchquert sowohl den Nucleus accumbens (NAcc), als auch die ventrale Spitze des Kopfs des Nucleus caudatus (CN), dringt in die weiße Substanz des medialen präfrontalen Kortex vor und endet am Pol des orbitofrontalen Kortex (OFC).

Während Verbindungen von BNST und NAcc wiederholt beschrieben wurden, liegen bisher keine Berichte über Verbindungen von BNST und CN vor. Sie stehen jedoch im Einklang mit Beschreibungen des internen Konnektivitätsprofils des CN, welches im Kopf des CN ein deutliches Übergewicht anteroposteriorer Faserverläufe aufweist. Diese Verbindungen könnten darauf hinweisen, dass Teile des CN, ähnlich wie der NAcc, an limbischen Funktionen beteiligt sind.

Während strukturelle Verbindungen von BNST und OFC bislang nicht beschrieben wurden, konnte funktionelle Konnektivität der beiden Strukturen in Studien sowohl an Affen, als auch an Menschen gezeigt werden. Die Integrität einer solchen Verbindung könnte eine wichtige Rolle in der Pathophysiologie von Angststörungen spielen, wobei der BNST möglicherweise als Schaltstelle zwischen OFC, Amygdala, PVH und weiteren Strukturen fungiert.

Die vorliegenden Studienergebnisse zeigen nur sporadisch Verbindungen zwischen BNST und Hirnstamm. Solche Verbindungen wurden vielfach in Tieren beschrieben, weshalb anzunehmen ist, dass dieses Ergebnis auf technische Limitationen des PFT zurück zu führen ist. Tatsächlich führte eine Vergrößerung des maximal erlaubten Winkels dazu, dass in deutlich mehr Probandendaten entsprechende Verbindungen gefunden werden konnten. Diese erwiesen sich

jedoch als sehr unspezifisch mit hoher interindividueller Variabilität, weshalb eine zuverlässige Abgrenzung von falsch positiven Ergebnissen kaum möglich ist.

Bibliography

1. Abramovich, D.R. and P. Rowe, *Foetal plasma testosterone levels at mid-pregnancy and at term: relationship to foetal sex.* J Endocrinol, 1973. **56**(3): p. 621-2.
2. Aghajani, M., I.M. Veer, M.J. van Tol, A. Aleman, M.A. van Buchem, D.J. Veltman, S.A. Rombouts, and N.J. van der Wee, *Neuroticism and extraversion are associated with amygdala resting-state functional connectivity.* Cogn Affect Behav Neurosci, 2013.
3. Alden, M., J.M. Besson, and J.F. Bernard, *Organization of the efferent projections from the pontine parabrachial area to the bed nucleus of the stria terminalis and neighboring regions: a PHA-L study in the rat.* J Comp Neurol, 1994. **341**(3): p. 289-314.
4. Alexander, A.L., J.E. Lee, M. Lazar, and A.S. Field, *Diffusion tensor imaging of the brain.* Neurotherapeutics, 2007. **4**(3): p. 316-29.
5. Alheid, G.F. and L. Heimer, *New perspectives in basal forebrain organization of special relevance for neuropsychiatric disorders: the striatopallidal, amygdaloid, and corticopetal components of substantia innominata.* Neuroscience, 1988. **27**(1): p. 1-39.
6. Alheid, G.F., J. De Olmos, and C.A. Beltramino, *Amygdala and extended amygdala*, in *The Rat Nervous System*, G. Paxinos, Editor. 1995, Academic Press: Orlando, FL. p. 495-578.
7. Alheid, G.F., C.A. Beltramino, J.S. De Olmos, M.S. Forbes, D.J. Swanson, and L. Heimer, *The neuronal organization of the supracapsular part of the stria terminalis in the rat: the dorsal component of the extended amygdala.* Neuroscience, 1998. **84**(4): p. 967-96.
8. Alheid, G.F., S.J. Shammah-Lagnado, and C.A. Beltramino, *The interstitial nucleus of the posterior limb of the anterior commissure: a novel layer of the central division of extended amygdala.* Ann N Y Acad Sci, 1999. **877**: p. 645-54.
9. Allen, L.S., M. Hines, J.E. Shryne, and R.A. Gorski, *Two sexually dimorphic cell groups in the human brain.* J Neurosci, 1989. **9**(2): p. 497-506.
10. Allen, L.S. and R.A. Gorski, *Sex difference in the bed nucleus of the stria terminalis of the human brain.* J Comp Neurol, 1990. **302**(4): p. 697-706.
11. Alvarez, R.P., G. Chen, J. Bodurka, R. Kaplan, and C. Grillon, *Phasic and sustained fear in humans elicits distinct patterns of brain activity.* Neuroimage, 2011. **55**(1): p. 389-400.
12. Anand, B.K. and J.R. Brobeck, *Hypothalamic control of food intake in rats and cats.* Yale J Biol Med, 1951. **24**(2): p. 123-40.
13. Andersson, J. *eddy -- a tool for correcting eddy currents and movements in diffusion data*. 2013 20.12.2013]; Available from: http://fsl.fmrib.ox.ac.uk/fsl/fslwiki/EDDY.
14. Andy, O.J. and H. Stephan, *The septum in the human brain.* J Comp Neurol, 1968. **133**(3): p. 383-410.
15. Angeles-Castellanos, M., J. Mendoza, and C. Escobar, *Restricted feeding schedules phase shift daily rhythms of c-Fos and protein Per1*

immunoreactivity in corticolimbic regions in rats. Neuroscience, 2007. **144**(1): p. 344-55.
16. Arluison, M., G. Brochier, M. Vankova, V. Leviel, J. Villalobos, and G. Tramu, *Demonstration of peptidergic afferents to the bed nucleus of the stria terminalis using local injections of colchicine. A combined immunohistochemical and retrograde tracing study.* Brain Res Bull, 1994. **34**(4): p. 319-37.
17. Ashburner, J. and K.J. Friston, *Unified segmentation.* Neuroimage, 2005. **26**(3): p. 839-51.
18. Assaf, Y., R.Z. Freidlin, G.K. Rohde, and P.J. Basser, *New modeling and experimental framework to characterize hindered and restricted water diffusion in brain white matter.* Magn Reson Med, 2004. **52**(5): p. 965-78.
19. Aston-Jones, G., J.M. Delfs, J. Druhan, and Y. Zhu, *The bed nucleus of the stria terminalis. A target site for noradrenergic actions in opiate withdrawal.* Ann N Y Acad Sci, 1999. **877**: p. 486-98.
20. Avery, S.N., T.A. Thornton-Wells, A.W. Anderson, and J.U. Blackford, *White matter integrity deficits in prefrontal-amygdala pathways in Williams syndrome.* Neuroimage, 2012. **59**(2): p. 887-94.
21. Avery, S.N., J.A. Clauss, D.G. Winder, N. Woodward, S. Heckers, and J.U. Blackford, *BNST neurocircuitry in humans.* Neuroimage, 2014. **91**: p. 311-323.
22. Bähr, M. and M. Frotscher, *Neurologisch-topische Diagnostik: Anatomie - Funktion - Klinik*. 9. ed. 2009, Stuttgart: Thieme.
23. Bar-Shir, A. and Y. Cohen, *Crossing fibers, diffractions and nonhomogeneous magnetic field: correction of artifacts by bipolar gradient pulses.* Magn Reson Imaging, 2008. **26**(6): p. 801-8.
24. Basser, P.J., J. Mattiello, and D. LeBihan, *Estimation of the effective self-diffusion tensor from the NMR spin echo.* J Magn Reson B, 1994. **103**(3): p. 247-54.
25. Basser, P.J., J. Mattiello, and D. LeBihan, *MR diffusion tensor spectroscopy and imaging.* Biophys J, 1994. **66**(1): p. 259-67.
26. Basser, P.J. and C. Pierpaoli, *Microstructural and physiological features of tissues elucidated by quantitative-diffusion-tensor MRI.* J Magn Reson B, 1996. **111**(3): p. 209-19.
27. Baur, V., A.B. Bruhl, U. Herwig, T. Eberle, M. Rufer, A. Delsignore, L. Jancke, and J. Hanggi, *Evidence of frontotemporal structural hypoconnectivity in social anxiety disorder: A quantitative fiber tractography study.* Hum Brain Mapp, 2013. **34**(2): p. 437-46.
28. Beal, M.F., D.W. Ellison, M.F. Mazurek, K.J. Swartz, J.R. Malloy, E.D. Bird, and J.B. Martin, *A detailed examination of substance P in pathologically graded cases of Huntington's disease.* J Neurol Sci, 1988. **84**(1): p. 51-61.
29. Beal, M.F., M.F. Mazurek, D.W. Ellison, K.J. Swartz, U. McGarvey, E.D. Bird, and J.B. Martin, *Somatostatin and neuropeptide Y concentrations in pathologically graded cases of Huntington's disease.* Ann Neurol, 1988. **23**(6): p. 562-9.
30. Beaulieu, C., *The basis of anisotropic water diffusion in the nervous system - a technical review.* NMR Biomed, 2002. **15**(7-8): p. 435-55.

31. Behrens, T.E., M.W. Woolrich, M. Jenkinson, H. Johansen-Berg, R.G. Nunes, S. Clare, P.M. Matthews, J.M. Brady, and S.M. Smith, *Characterization and propagation of uncertainty in diffusion-weighted MR imaging.* Magn Reson Med, 2003. **50**(5): p. 1077-88.
32. Behrens, T.E., H.J. Berg, S. Jbabdi, M.F. Rushworth, and M.W. Woolrich, *Probabilistic diffusion tractography with multiple fibre orientations: What can we gain?* Neuroimage, 2007. **34**(1): p. 144-55.
33. Bienkowski, M.S. and L. Rinaman, *Immune challenge activates neural inputs to the ventrolateral bed nucleus of the stria terminalis.* Physiol Behav, 2011. **104**(2): p. 257-65.
34. Bienkowski, M.S. and L. Rinaman, *Common and distinct neural inputs to the medial central nucleus of the amygdala and anterior ventrolateral bed nucleus of stria terminalis in rats.* Brain Struct Funct, 2013. **218**(1): p. 187-208.
35. Bingham, B., C. Myung, L. Innala, M. Gray, A. Anonuevo, and V. Viau, *Androgen receptors in the posterior bed nucleus of the stria terminalis increase neuropeptide expression and the stress-induced activation of the paraventricular nucleus of the hypothalamus.* Neuropsychopharmacology, 2011. **36**(7): p. 1433-43.
36. Boehme, S., V. Ritter, S. Tefikow, U. Stangier, B. Strauss, W.H. Miltner, and T. Straube, *Brain activation during anticipatory anxiety in social anxiety disorder.* Soc Cogn Affect Neurosci, 2013.
37. Brockhaus, H., *Zur feineren Anatomie des Septum und des Striatum.* J Psychol Neurol, 1942. **51**(1-2): p. 1-56.
38. Brureau, A., C. Zussy, B. Delair, C. Ogier, G. Ixart, T. Maurice, and L. Givalois, *Deregulation of hypothalamic-pituitary-adrenal axis functions in an Alzheimer's disease rat model.* Neurobiol Aging, 2013. **34**(5): p. 1426-39.
39. Buffalari, D.M. and R.E. See, *Inactivation of the bed nucleus of the stria terminalis in an animal model of relapse: effects on conditioned cue-induced reinstatement and its enhancement by yohimbine.* Psychopharmacology (Berl), 2011. **213**(1): p. 19-27.
40. Canteras, N.S., R.B. Simerly, and L.W. Swanson, *Connections of the posterior nucleus of the amygdala.* J Comp Neurol, 1992. **324**(2): p. 143-79.
41. Canteras, N.S. and L.W. Swanson, *Projections of the ventral subiculum to the amygdala, septum, and hypothalamus: a PHAL anterograde tract-tracing study in the rat.* J Comp Neurol, 1992. **324**(2): p. 180-94.
42. Canteras, N.S., R.B. Simerly, and L.W. Swanson, *Organization of projections from the medial nucleus of the amygdala: a PHAL study in the rat.* J Comp Neurol, 1995. **360**(2): p. 213-45.
43. Carr, H.Y. and E.M. Purcell, *Effects of Diffusion on Free Precession in Nuclear Magnetic Resonance Experiments.* Phys. Rev., 1954. **94**: p. 630-638.
44. Cechetto, D.F., *Identification of a cortical site for stress-induced cardiovascular dysfunction.* Integr Physiol Behav Sci, 1994. **29**(4): p. 362-73.

45. Cheal, M.L. and R.L. Sprott, *Social olfaction: a review of the role of olfaction in a variety of animal behaviors.* Psychol Rep, 1971. **29**(1): p. 195-243.
46. Chen, H.C., D.Y. Chen, C.C. Chen, and K.C. Liang, *Pre- and post-training infusion of prazosin into the bed nucleus of the stria terminalis impaired acquisition and retention in a Morris water maze task.* Chin J Physiol, 2004. **47**(1): p. 49-59.
47. Chiba, T., T. Kayahara, and K. Nakano, *Efferent projections of infralimbic and prelimbic areas of the medial prefrontal cortex in the Japanese monkey, Macaca fuscata.* Brain Res, 2001. **888**(1): p. 83-101.
48. Choi, C.Y., S.R. Han, G.T. Yee, and C.H. Lee, *Central core of the cerebrum.* J Neurosurg, 2011. **114**(2): p. 463-9.
49. Choi, D.C., A.R. Furay, N.K. Evanson, M.M. Ostrander, Y.M. Ulrich-Lai, and J.P. Herman, *Bed nucleus of the stria terminalis subregions differentially regulate hypothalamic-pituitary-adrenal axis activity: implications for the integration of limbic inputs.* J Neurosci, 2007. **27**(8): p. 2025-34.
50. Choi, J.M., S. Padmala, and L. Pessoa, *Impact of state anxiety on the interaction between threat monitoring and cognition.* Neuroimage, 2012. **59**(2): p. 1912-23.
51. Choi, J.M., S. Padmala, P. Spechler, and L. Pessoa, *Pervasive competition between threat and reward in the brain.* Soc Cogn Affect Neurosci, 2013.
52. Chung, W.C., G.J. De Vries, and D.F. Swaab, *Sexual differentiation of the bed nucleus of the stria terminalis in humans may extend into adulthood.* J Neurosci, 2002. **22**(3): p. 1027-33.
53. Ciccocioppo, R., M. Biondini, L. Antonelli, J. Wichmann, F. Jenck, and M. Massi, *Reversal of stress- and CRF-induced anorexia in rats by the synthetic nociceptin/orphanin FQ receptor agonist, Ro 64-6198.* Psychopharmacology (Berl), 2002. **161**(2): p. 113-9.
54. Ciccocioppo, R., A. Fedeli, D. Economidou, F. Policani, F. Weiss, and M. Massi, *The bed nucleus is a neuroanatomical substrate for the anorectic effect of corticotropin-releasing factor and for its reversal by nociceptin/orphanin FQ.* J Neurosci, 2003. **23**(28): p. 9445-51.
55. Ciccocioppo, R., A. Cippitelli, D. Economidou, A. Fedeli, and M. Massi, *Nociceptin/orphanin FQ acts as a functional antagonist of corticotropin-releasing factor to inhibit its anorectic effect.* Physiol Behav, 2004. **82**(1): p. 63-8.
56. Conrad, K.L., K.M. Louderback, C.P. Gessner, and D.G. Winder, *Stress-induced alterations in anxiety-like behavior and adaptations in plasticity in the bed nucleus of the stria terminalis.* Physiol Behav, 2011. **104**(2): p. 248-56.
57. Conturo, T.E., R.C. McKinstry, E. Akbudak, and B.H. Robinson, *Encoding of anisotropic diffusion with tetrahedral gradients: a general mathematical diffusion formalism and experimental results.* Magn Reson Med, 1996. **35**(3): p. 399-412.

58. Crestani, C.C., F.H. Alves, L.B. Resstel, and F.M. Correa, *The bed nucleus of the stria terminalis modulates exercise-evoked cardiovascular responses in rats.* Exp Physiol, 2010. **95**(1): p. 69-79.
59. Crestani, C.C., F.H. Alves, F.V. Gomes, L.B. Resstel, F.M. Correa, and J.P. Herman, *Mechanisms in the bed nucleus of the stria terminalis involved in control of autonomic and neuroendocrine functions: a review.* Curr Neuropharmacol, 2013. **11**(2): p. 141-59.
60. Cullinan, W.E., J.P. Herman, and S.J. Watson, *Ventral subicular interaction with the hypothalamic paraventricular nucleus: evidence for a relay in the bed nucleus of the stria terminalis.* J Comp Neurol, 1993. **332**(1): p. 1-20.
61. Dabrowska, J., R. Hazra, T.H. Ahern, J.D. Guo, A.J. McDonald, F. Mascagni, J.F. Muller, L.J. Young, and D.G. Rainnie, *Neuroanatomical evidence for reciprocal regulation of the corticotrophin-releasing factor and oxytocin systems in the hypothalamus and the bed nucleus of the stria terminalis of the rat: Implications for balancing stress and affect.* Psychoneuroendocrinology, 2011. **36**(9): p. 1312-26.
62. Davis, M., D.L. Walker, and Y. Lee, *Roles of the amygdala and bed nucleus of the stria terminalis in fear and anxiety measured with the acoustic startle reflex. Possible relevance to PTSD.* Ann N Y Acad Sci, 1997. **821**: p. 305-31.
63. Davis, M. and C. Shi, *The extended amygdala: are the central nucleus of the amygdala and the bed nucleus of the stria terminalis differentially involved in fear versus anxiety?* Ann N Y Acad Sci, 1999. **877**: p. 281-91.
64. Davis, M., D.L. Walker, L. Miles, and C. Grillon, *Phasic vs sustained fear in rats and humans: role of the extended amygdala in fear vs anxiety.* Neuropsychopharmacology, 2010. **35**(1): p. 105-35.
65. de Olmos, J.S. and W.R. Ingram, *The projection field of the stria terminalis in the rat brain. An experimental study.* J Comp Neurol, 1972. **146**(3): p. 303-34.
66. de Olmos, J.S., G.F. Alheid, and C.A. Beltramino, *Amygdala*, in *The Rat Nervous System*, G. Paxinos, Editor. 1985, Academic: Sydney. p. 223-334.
67. de Olmos, J.S., *Amygdala*, in *The Human nervous system*, G. Paxinos, Editor. 1990, Academic Press: San Diego. p. 583-710.
68. Deak, T., K.T. Nguyen, A.L. Ehrlich, L.R. Watkins, R.L. Spencer, S.F. Maier, J. Licinio, M.L. Wong, G.P. Chrousos, E. Webster, and P.W. Gold, *The impact of the nonpeptide corticotropin-releasing hormone antagonist antalarmin on behavioral and endocrine responses to stress.* Endocrinology, 1999. **140**(1): p. 79-86.
69. Deary, I.J., M.E. Bastin, A. Pattie, J.D. Clayden, L.J. Whalley, J.M. Starr, and J.M. Wardlaw, *White matter integrity and cognition in childhood and old age.* Neurology, 2006. **66**(4): p. 505-12.
70. del Abril, A., S. Segovia, and A. Guillamon, *The bed nucleus of the stria terminalis in the rat: regional sex differences controlled by gonadal steroids early after birth.* Brain Res, 1987. **429**(2): p. 295-300.

71. Delfs, J.M., Y. Zhu, J.P. Druhan, and G. Aston-Jones, *Noradrenaline in the ventral forebrain is critical for opiate withdrawal-induced aversion.* Nature, 2000. **403**(6768): p. 430-4.
72. Delgado, J.M. and B.K. Anand, *Increase of food intake induced by electrical stimulation of the lateral hypothalamus.* Am J Physiol, 1953. **172**(1): p. 162-8.
73. Desikan, R.S., F. Segonne, B. Fischl, B.T. Quinn, B.C. Dickerson, D. Blacker, R.L. Buckner, A.M. Dale, R.P. Maguire, B.T. Hyman, M.S. Albert, and R.J. Killiany, *An automated labeling system for subdividing the human cerebral cortex on MRI scans into gyral based regions of interest.* Neuroimage, 2006. **31**(3): p. 968-80.
74. Devine, D.P., S.J. Watson, and H. Akil, *Nociceptin/orphanin FQ regulates neuroendocrine function of the limbic-hypothalamic-pituitary-adrenal axis.* Neuroscience, 2001. **102**(3): p. 541-53.
75. Devor, M., *Components of mating dissociated by lateral olfactory tract transection in male hamsters.* Brain Res, 1973. **64**: p. 437-41.
76. Deyama, S., S. Ide, N. Kondoh, T. Yamaguchi, M. Yoshioka, and M. Minami, *Inhibition of noradrenaline release by clonidine in the ventral bed nucleus of the stria terminalis attenuates pain-induced aversion in rats.* Neuropharmacology, 2011. **61**(1-2): p. 156-60.
77. Dong, H.W., G.D. Petrovich, A.G. Watts, and L.W. Swanson, *Basic organization of projections from the oval and fusiform nuclei of the bed nuclei of the stria terminalis in adult rat brain.* J Comp Neurol, 2001. **436**(4): p. 430-55.
78. Dong, H.W., G.D. Petrovich, and L.W. Swanson, *Topography of projections from amygdala to bed nuclei of the stria terminalis.* Brain Res Brain Res Rev, 2001. **38**(1-2): p. 192-246.
79. Dong, H.W. and L.W. Swanson, *Projections from the rhomboid nucleus of the bed nuclei of the stria terminalis: implications for cerebral hemisphere regulation of ingestive behaviors.* J Comp Neurol, 2003. **463**(4): p. 434-72.
80. Dong, H.W. and L.W. Swanson, *Organization of axonal projections from the anterolateral area of the bed nuclei of the stria terminalis.* J Comp Neurol, 2004. **468**(2): p. 277-98.
81. Dong, H.W. and L.W. Swanson, *Projections from bed nuclei of the stria terminalis, posterior division: implications for cerebral hemisphere regulation of defensive and reproductive behaviors.* J Comp Neurol, 2004. **471**(4): p. 396-433.
82. Dong, H.W. and L.W. Swanson, *Projections from bed nuclei of the stria terminalis, dorsomedial nucleus: implications for cerebral hemisphere integration of neuroendocrine, autonomic, and drinking responses.* J Comp Neurol, 2006. **494**(1): p. 75-107.
83. Dunn, J.D., *Plasma corticosterone responses to electrical stimulation of the bed nucleus of the stria terminalis.* Brain Res, 1987. **407**(2): p. 327-31.
84. Dunn, J.D. and T.J. Williams, *Cardiovascular responses to electrical stimulation of the bed nucleus of the stria terminalis.* J Comp Neurol, 1995. **352**(2): p. 227-34.

85. Duvarci, S., E.P. Bauer, and D. Pare, *The bed nucleus of the stria terminalis mediates inter-individual variations in anxiety and fear.* J Neurosci, 2009. **29**(33): p. 10357-61.
86. Eiler, W.J., 2nd, R. Seyoum, K.L. Foster, C. Mailey, and H.L. June, *D1 dopamine receptor regulates alcohol-motivated behaviors in the bed nucleus of the stria terminalis in alcohol-preferring (P) rats.* Synapse, 2003. **48**(1): p. 45-56.
87. Emery, D.E. and B.D. Sachs, *Copulatory behavior in male rats with lesions in the bed nucleus of the stria terminalis.* Physiol Behav, 1976. **17**(5): p. 803-6.
88. Epping-Jordan, M.P., A. Markou, and G.F. Koob, *The dopamine D-1 receptor antagonist SCH 23390 injected into the dorsolateral bed nucleus of the stria terminalis decreased cocaine reinforcement in the rat.* Brain Res, 1998. **784**(1-2): p. 105-15.
89. Erb, S., Y. Shaham, and J. Stewart, *Stress-induced relapse to drug seeking in the rat: role of the bed nucleus of the stria terminalis and amygdala.* Stress, 2001. **4**(4): p. 289-303.
90. Fedorov, A., R. Beichel, J. Kalpathy-Cramer, J. Finet, J.C. Fillion-Robin, S. Pujol, C. Bauer, D. Jennings, F. Fennessy, M. Sonka, J. Buatti, S. Aylward, J.V. Miller, S. Pieper, and R. Kikinis, *3D Slicer as an image computing platform for the Quantitative Imaging Network.* Magn Reson Imaging, 2012. **30**(9): p. 1323-41.
91. Figueiredo, H.F., A. Bruestle, B. Bodie, C.M. Dolgas, and J.P. Herman, *The medial prefrontal cortex differentially regulates stress-induced c-fos expression in the forebrain depending on type of stressor.* Eur J Neurosci, 2003. **18**(8): p. 2357-64.
92. Fliers, E., S.E. Guldenaar, N. van de Wal, and D.F. Swaab, *Extrahypothalamic vasopressin and oxytocin in the human brain; presence of vasopressin cells in the bed nucleus of the stria terminalis.* Brain Res, 1986. **375**(2): p. 363-7.
93. Floyd, N.S., J.L. Price, A.T. Ferry, K.A. Keay, and R. Bandler, *Orbitomedial prefrontal cortical projections to hypothalamus in the rat.* J Comp Neurol, 2001. **432**(3): p. 307-28.
94. Fox, A.S., S.E. Shelton, T.R. Oakes, R.J. Davidson, and N.H. Kalin, *Trait-like brain activity during adolescence predicts anxious temperament in primates.* PLoS One, 2008. **3**(7): p. e2570.
95. Fox, A.S., S.E. Shelton, T.R. Oakes, A.K. Converse, R.J. Davidson, and N.H. Kalin, *Orbitofrontal cortex lesions alter anxiety-related activity in the primate bed nucleus of stria terminalis.* J Neurosci, 2010. **30**(20): p. 7023-7.
96. Fox, C.A., *Certain basal telencephalic centers in the cat.* J Comp Neurol, 1940. **72**(1): p. 1-62.
97. Francesconi, W., F. Berton, G.F. Koob, and P.P. Sanna, *Intrinsic neuronal plasticity in the juxtacapsular nucleus of the bed nuclei of the stria terminalis (jcBNST).* Prog Neuropsychopharmacol Biol Psychiatry, 2009. **33**(8): p. 1347-55.
98. Gaspar, P., B. Berger, C. Alvarez, A. Vigny, and J.P. Henry, *Catecholaminergic innervation of the septal area in man:*

immunocytochemical study using TH and DBH antibodies. J Comp Neurol, 1985. **241**(1): p. 12-33.
99. Gaspar, P., C. Duyckaerts, A. Febvret, R. Benoit, B. Beck, and B. Berger, *Subpopulations of somatostatin 28-immunoreactive neurons display different vulnerability in senile dementia of the Alzheimer type.* Brain Res, 1989. **490**(1): p. 1-13.
100. Geeraedts, L.M., R. Nieuwenhuys, and J.G. Veening, *Medial forebrain bundle of the rat: III. Cytoarchitecture of the rostral (telencephalic) part of the medial forebrain bundle bed nucleus.* J Comp Neurol, 1990. **294**(4): p. 507-36.
101. George, O., C. Sanders, J. Freiling, E. Grigoryan, S. Vu, C.D. Allen, E. Crawford, C.D. Mandyam, and G.F. Koob, *Recruitment of medial prefrontal cortex neurons during alcohol withdrawal predicts cognitive impairment and excessive alcohol drinking.* Proc Natl Acad Sci U S A, 2012. **109**(44): p. 18156-61.
102. Georges, F. and G. Aston-Jones, *Potent regulation of midbrain dopamine neurons by the bed nucleus of the stria terminalis.* J Neurosci, 2001. **21**(16): p. RC160.
103. Georges, F. and G. Aston-Jones, *Activation of ventral tegmental area cells by the bed nucleus of the stria terminalis: a novel excitatory amino acid input to midbrain dopamine neurons.* J Neurosci, 2002. **22**(12): p. 5173-87.
104. Gilks, W.R., S. Richardson, and D.J. Spiegelhalter, *Markov chain Monte Carlo in practice*. 1998, Boca Raton, Fla.: Chapman & Hall. xvii, 486 p.
105. Gold, A.L., R.A. Morey, and G. McCarthy, *Amygdala-prefrontal cortex functional connectivity during threat-induced anxiety and goal distraction.* Biol Psychiatry, 2015. **77**(4): p. 394-403.
106. Gray, H. and W.H. Lewis. *Anatomy of the human body*. 1918 28.11.13]; 20th:[Available from: http://www.bartelby.com/107/191.html.
107. Gray, M.A. and H.D. Critchley, *Interoceptive basis to craving.* Neuron, 2007. **54**(2): p. 183-6.
108. Gray, T.S. and D.J. Magnuson, *Neuropeptide neuronal efferents from the bed nucleus of the stria terminalis and central amygdaloid nucleus to the dorsal vagal complex in the rat.* J Comp Neurol, 1987. **262**(3): p. 365-74.
109. Gray, T.S., R.A. Piechowski, J.M. Yracheta, P.A. Rittenhouse, C.L. Bethea, and L.D. Van de Kar, *Ibotenic acid lesions in the bed nucleus of the stria terminalis attenuate conditioned stress-induced increases in prolactin, ACTH and corticosterone.* Neuroendocrinology, 1993. **57**(3): p. 517-24.
110. Grupe, D.W., D.J. Oathes, and J.B. Nitschke, *Dissecting the anticipation of aversion reveals dissociable neural networks.* Cereb Cortex, 2013. **23**(8): p. 1874-83.
111. Gungor, N.Z. and D. Pare, *CGRP inhibits neurons of the bed nucleus of the stria terminalis: implications for the regulation of fear and anxiety.* J Neurosci, 2014. **34**(1): p. 60-5.
112. Haber, S.N. and W.J. Nauta, *Ramifications of the globus pallidus in the rat as indicated by patterns of immunohistochemistry.* Neuroscience, 1983. **9**(2): p. 245-60.

113. Haber, S.N. and B. Knutson, *The reward circuit: linking primate anatomy and human imaging.* Neuropsychopharmacology, 2010. **35**(1): p. 4-26.
114. Hahn, A., P. Stein, C. Windischberger, A. Weissenbacher, C. Spindelegger, E. Moser, S. Kasper, and R. Lanzenberger, *Reduced resting-state functional connectivity between amygdala and orbitofrontal cortex in social anxiety disorder.* Neuroimage, 2011. **56**(3): p. 881-9.
115. Hahn, E.L., *Spin Echoes.* Phys. Rev., 1950. **50**: p. 580-594.
116. Hamilton, R.B., H. Ellenberger, D. Liskowsky, and N. Schneiderman, *Parabrachial area as mediator of bradycardia in rabbits.* J Auton Nerv Syst, 1981. **4**(3): p. 261-81.
117. Hammack, S.E., J.D. Guo, R. Hazra, J. Dabrowska, K.M. Myers, and D.G. Rainnie, *The response of neurons in the bed nucleus of the stria terminalis to serotonin: implications for anxiety.* Prog Neuropsychopharmacol Biol Psychiatry, 2009. **33**(8): p. 1309-20.
118. Harris, G.C. and G. Aston-Jones, *Critical role for ventral tegmental glutamate in preference for a cocaine-conditioned environment.* Neuropsychopharmacology, 2003. **28**(1): p. 73-6.
119. Hasan, K.M., D.L. Parker, and A.L. Alexander, *Comparison of gradient encoding schemes for diffusion-tensor MRI.* J Magn Reson Imaging, 2001. **13**(5): p. 769-80.
120. Hebda-Bauer, E.K., T.A. Simmons, A. Sugg, E. Ural, J.A. Stewart, J.L. Beals, Q. Wei, S.J. Watson, and H. Akil, *3xTg-AD mice exhibit an activated central stress axis during early-stage pathology.* J Alzheimers Dis, 2013. **33**(2): p. 407-22.
121. Heimer, L., *Basal forebrain in the context of schizophrenia.* Brain Res Brain Res Rev, 2000. **31**(2-3): p. 205-35.
122. Herman, J.P., W.E. Cullinan, and S.J. Watson, *Involvement of the bed nucleus of the stria terminalis in tonic regulation of paraventricular hypothalamic CRH and AVP mRNA expression.* J Neuroendocrinol, 1994. **6**(4): p. 433-42.
123. Herman, J.P. and W.E. Cullinan, *Neurocircuitry of stress: central control of the hypothalamo-pituitary-adrenocortical axis.* Trends Neurosci, 1997. **20**(2): p. 78-84.
124. Herwig, U., T. Baumgartner, T. Kaffenberger, A. Bruhl, M. Kottlow, U. Schreiter-Gasser, B. Abler, L. Jancke, and M. Rufer, *Modulation of anticipatory emotion and perception processing by cognitive control.* Neuroimage, 2007. **37**(2): p. 652-62.
125. Hines, M., L.S. Allen, and R.A. Gorski, *Sex differences in subregions of the medial nucleus of the amygdala and the bed nucleus of the stria terminalis of the rat.* Brain Res, 1992. **579**(2): p. 321-6.
126. Hirooka, Y., J.W. Polson, P.D. Potts, and R.A. Dampney, *Hypoxia-induced Fos expression in neurons projecting to the pressor region in the rostral ventrolateral medulla.* Neuroscience, 1997. **80**(4): p. 1209-24.
127. Holmes, C.J., R. Hoge, L. Collins, R. Woods, A.W. Toga, and A.C. Evans, *Enhancement of MR images using registration for signal averaging.* J Comput Assist Tomogr, 1998. **22**(2): p. 324-33.

128. Holstege, G., L. Meiners, and K. Tan, *Projections of the bed nucleus of the stria terminalis to the mesencephalon, pons, and medulla oblongata in the cat.* Exp Brain Res, 1985. **58**(2): p. 379-91.
129. Hope, T., L.T. Westlye, and A. Bjornerud, *The effect of gradient sampling schemes on diffusion metrics derived from probabilistic analysis and tract-based spatial statistics.* Magn Reson Imaging, 2012. **30**(3): p. 402-12.
130. Hugenschmidt, C.E., A.M. Peiffer, R.A. Kraft, R. Casanova, A.R. Deibler, J.H. Burdette, J.A. Maldjian, and P.J. Laurienti, *Relating imaging indices of white matter integrity and volume in healthy older adults.* Cereb Cortex, 2008. **18**(2): p. 433-42.
131. Hurley, K.M., H. Herbert, M.M. Moga, and C.B. Saper, *Efferent projections of the infralimbic cortex of the rat.* J Comp Neurol, 1991. **308**(2): p. 249-76.
132. Hyytia, P. and G.F. Koob, *GABAA receptor antagonism in the extended amygdala decreases ethanol self-administration in rats.* Eur J Pharmacol, 1995. **283**(1-3): p. 151-9.
133. Ide, S., T. Hara, A. Ohno, R. Tamano, K. Koseki, T. Naka, C. Maruyama, K. Kaneda, M. Yoshioka, and M. Minami, *Opposing roles of corticotropin-releasing factor and neuropeptide Y within the dorsolateral bed nucleus of the stria terminalis in the negative affective component of pain in rats.* J Neurosci, 2013. **33**(14): p. 5881-94.
134. Inui, T., C. Inui-Yamamoto, Y. Yoshioka, I. Ohzawa, and T. Shimura, *Activation of efferents from the basolateral amygdala during the retrieval of conditioned taste aversion.* Neurobiol Learn Mem, 2013. **106**: p. 210-20.
135. Iwasaki, H., E. Jodo, A. Kawauchi, T. Miki, Y. Kayama, and Y. Koyama, *Role of the lateral preoptic area and the bed nucleus of stria terminalis in the regulation of penile erection.* Brain Res, 2010. **1357**: p. 70-8.
136. Jahanfar, S., C.H. Awang, R.A. Rahman, R.D. Samsuddin, and C.P. See, *Is 3alpha-androstenol pheromone related to menstrual synchrony?* J Fam Plann Reprod Health Care, 2007. **33**(2): p. 116-8.
137. Jalabert, M., G. Aston-Jones, E. Herzog, O. Manzoni, and F. Georges, *Role of the bed nucleus of the stria terminalis in the control of ventral tegmental area dopamine neurons.* Prog Neuropsychopharmacol Biol Psychiatry, 2009. **33**(8): p. 1336-46.
138. Jennings, J.H., D.R. Sparta, A.M. Stamatakis, R.L. Ung, K.E. Pleil, T.L. Kash, and G.D. Stuber, *Distinct extended amygdala circuits for divergent motivational states.* Nature, 2013. **496**(7444): p. 224-8.
139. Jennings, J.H., G. Rizzi, A.M. Stamatakis, R.L. Ung, and G.D. Stuber, *The inhibitory circuit architecture of the lateral hypothalamus orchestrates feeding.* Science, 2013. **341**(6153): p. 1517-21.
140. Jones, D.K., M.A. Horsfield, and A. Simmons, *Optimal strategies for measuring diffusion in anisotropic systems by magnetic resonance imaging.* Magn Reson Med, 1999. **42**(3): p. 515-25.
141. Jones, D.K., *The effect of gradient sampling schemes on measures derived from diffusion tensor MRI: a Monte Carlo study.* Magn Reson Med, 2004. **51**(4): p. 807-15.

142. Kalin, N.H. and L.K. Takahashi, *Fear-motivated behavior induced by prior shock experience is mediated by corticotropin-releasing hormone systems.* Brain Res, 1990. **509**(1): p. 80-4.
143. Kapp, B.S., J.S. Schwaber, and P.A. Driscoll, *Frontal cortex projections to the amygdaloid central nucleus in the rabbit.* Neuroscience, 1985. **15**(2): p. 327-46.
144. Karampinos, D.C., A.T. Van, W.C. Olivero, J.G. Georgiadis, and B.P. Sutton, *High-resolution diffusion tensor imaging of the human pons with a reduced field-of-view, multishot, variable-density, spiral acquisition at 3 T.* Magn Reson Med, 2009. **62**(4): p. 1007-16.
145. Kelley, A.E., V.B. Domesick, and W.J. Nauta, *The amygdalostriatal projection in the rat--an anatomical study by anterograde and retrograde tracing methods.* Neuroscience, 1982. **7**(3): p. 615-30.
146. Khachaturian, M.H., J.J. Wisco, and D.S. Tuch, *Boosting the sampling efficiency of q-Ball imaging using multiple wavevector fusion.* Magn Reson Med, 2007. **57**(2): p. 289-96.
147. Kim, M.J. and P.J. Whalen, *The structural integrity of an amygdala-prefrontal pathway predicts trait anxiety.* J Neurosci, 2009. **29**(37): p. 11614-8.
148. Kim, S.Y., A. Adhikari, S.Y. Lee, J.H. Marshel, C.K. Kim, C.S. Mallory, M. Lo, S. Pak, J. Mattis, B.K. Lim, R.C. Malenka, M.R. Warden, R. Neve, K.M. Tye, and K. Deisseroth, *Diverging neural pathways assemble a behavioural state from separable features in anxiety.* Nature, 2013. **496**(7444): p. 219-23.
149. Klingler, J. and P. Gloor, *The connections of the amygdala and of the anterior temporal cortex in the human brain.* J Comp Neurol, 1960. **115**(3): p. 333-69.
150. Koay, C.G., L.C. Chang, J.D. Carew, C. Pierpaoli, and P.J. Basser, *A unifying theoretical and algorithmic framework for least squares methods of estimation in diffusion tensor imaging.* J Magn Reson, 2006. **182**(1): p. 115-25.
151. Koch, M. and D.G. Norris, *An assessment of eddy current sensitivity and correction in single-shot diffusion-weighted imaging.* Phys Med Biol, 2000. **45**(12): p. 3821-32.
152. Kotz, S.A., A. Anwander, H. Axer, and T.R. Knosche, *Beyond cytoarchitectonics: the internal and external connectivity structure of the caudate nucleus.* PLOS ONE, 2013. **8**(7): p. e70141.
153. Krettek, J.E. and J.L. Price, *Amygdaloid projections to subcortical structures within the basal forebrain and brainstem in the rat and cat.* J Comp Neurol, 1978. **178**(2): p. 225-54.
154. Krettek, J.E. and J.L. Price, *A description of the amygdaloid complex in the rat and cat with observations on intra-amygdaloid axonal connections.* J Comp Neurol, 1978. **178**(2): p. 255-80.
155. Krüger, O., T. Shiozawa, B. Kreifelts, K. Scheffler, and T. Ethofer, *Three distinct fiber pathways of the bed nucleus of the stria terminalis to the amygdala and prefrontal cortex.* Cortex, 2015. **66**: p. 60-68.

156. Kruijver, F.P., J.N. Zhou, C.W. Pool, M.A. Hofman, L.J. Gooren, and D.F. Swaab, *Male-to-female transsexuals have female neuron numbers in a limbic nucleus.* J Clin Endocrinol Metab, 2000. **85**(5): p. 2034-41.
157. Kudo, T., M. Uchigashima, T. Miyazaki, K. Konno, M. Yamasaki, Y. Yanagawa, M. Minami, and M. Watanabe, *Three types of neurochemical projection from the bed nucleus of the stria terminalis to the ventral tegmental area in adult mice.* J Neurosci, 2012. **32**(50): p. 18035-46.
158. Labuschagne, I., R. Jones, J. Callaghan, D. Whitehead, E.M. Dumas, M.J. Say, E.P. Hart, D. Justo, A. Coleman, R.C. Dar Santos, C. Frost, D. Craufurd, S.J. Tabrizi, J.C. Stout, and T.-H. Investigators, *Emotional face recognition deficits and medication effects in pre-manifest through stage-II Huntington's disease.* Psychiatry Res, 2013. **207**(1-2): p. 118-26.
159. Le Bihan, D., E. Breton, D. Lallemand, P. Grenier, E. Cabanis, and M. Laval-Jeantet, *MR imaging of intravoxel incoherent motions: application to diffusion and perfusion in neurologic disorders.* Radiology, 1986. **161**(2): p. 401-7.
160. Lee, Y. and M. Davis, *Role of the hippocampus, the bed nucleus of the stria terminalis, and the amygdala in the excitatory effect of corticotropin-releasing hormone on the acoustic startle reflex.* J Neurosci, 1997. **17**(16): p. 6434-46.
161. Lee, Y., S. Fitz, P.L. Johnson, and A. Shekhar, *Repeated stimulation of CRF receptors in the BNST of rats selectively induces social but not panic-like anxiety.* Neuropsychopharmacology, 2008. **33**(11): p. 2586-94.
162. Lehericy, S., M. Ducros, P.F. Van de Moortele, C. Francois, L. Thivard, C. Poupon, N. Swindale, K. Ugurbil, and D.S. Kim, *Diffusion tensor fiber tracking shows distinct corticostriatal circuits in humans.* Ann Neurol, 2004. **55**(4): p. 522-9.
163. Lehman, M.N. and S.S. Winans, *Evidence for a ventral non-strial pathway from the amygdala to the bed nucleus of the stria terminalis in the male golden hamster.* Brain Res, 1983. **268**(1): p. 139-46.
164. Lehman, M.N., J.B. Powers, and S.S. Winans, *Stria terminalis lesions alter the temporal pattern of copulatory behavior in the male golden hamster.* Behav Brain Res, 1983. **8**(1): p. 109-28.
165. Leichnetz, G.R. and J. Astruc, *The course of some prefrontal corticofugals to the pallidum, substantia innominata, and amygdaloid complex in monkeys.* Exp Neurol, 1977. **54**(1): p. 104-9.
166. Leri, F., J. Flores, D. Rodaros, and J. Stewart, *Blockade of stress-induced but not cocaine-induced reinstatement by infusion of noradrenergic antagonists into the bed nucleus of the stria terminalis or the central nucleus of the amygdala.* J Neurosci, 2002. **22**(13): p. 5713-8.
167. Lesur, A., P. Gaspar, C. Alvarez, and B. Berger, *Chemoanatomic compartments in the human bed nucleus of the stria terminalis.* Neuroscience, 1989. **32**(1): p. 181-94.
168. Levita, L., S.E. Hammack, I. Mania, X.Y. Li, M. Davis, and D.G. Rainnie, *5-hydroxytryptamine1A-like receptor activation in the bed nucleus of the stria terminalis: electrophysiological and behavioral studies.* Neuroscience, 2004. **128**(3): p. 583-96.

169. Levita, L., R. Hoskin, and S. Champi, *Avoidance of harm and anxiety: a role for the nucleus accumbens.* Neuroimage, 2012. **62**(1): p. 189-98.
170. Li, S. and G.J. Kirouac, *Projections from the paraventricular nucleus of the thalamus to the forebrain, with special emphasis on the extended amygdala.* J Comp Neurol, 2008. **506**(2): p. 263-87.
171. Li, X.F., Y.S. Lin, J.S. Kinsey-Jones, S.R. Milligan, S.L. Lightman, and K.T. O'Byrne, *The role of the bed nucleus of the stria terminalis in stress-induced inhibition of pulsatile luteinising hormone secretion in the female rat.* J Neuroendocrinol, 2011. **23**(1): p. 3-11.
172. Lübke, K.T., M. Hoenen, and B.M. Pause, *Differential processing of social chemosignals obtained from potential partners in regards to gender and sexual orientation.* Behav Brain Res, 2012. **228**(2): p. 375-87.
173. Lundström, J.N., J.A. Boyle, R.J. Zatorre, and M. Jones-Gotman, *Functional neuronal processing of body odors differs from that of similar common odors.* Cereb Cortex, 2008. **18**(6): p. 1466-74.
174. Luyten, L., C. Casteels, D. Vansteenwegen, K. van Kuyck, M. Koole, K. Van Laere, and B. Nuttin, *Micro-positron emission tomography imaging of rat brain metabolism during expression of contextual conditioning.* J Neurosci, 2012. **32**(1): p. 254-63.
175. Ma, S., S.W. Mifflin, J.T. Cunningham, and D.A. Morilak, *Chronic intermittent hypoxia sensitizes acute hypothalamic-pituitary-adrenal stress reactivity and Fos induction in the rat locus coeruleus in response to subsequent immobilization stress.* Neuroscience, 2008. **154**(4): p. 1639-47.
176. Ma, X., Y.M. Kadah, S.M. LaConte, and X. Hu, *Enhancing measured diffusion anisotropy in gray matter by eliminating CSF contamination with FLAIR.* Magn Reson Med, 2004. **51**(2): p. 423-7.
177. MacKay, D.J.C., *Probable Networks and Plausible Predictions - a Review of Practical Bayesian Methods for Supervised Neural Networks.* Network: Computation in Neural Systems, 1995. **6**(3): p. 469-505.
178. Madsen, H.B., R.M. Brown, J.L. Short, and A.J. Lawrence, *Investigation of the neuroanatomical substrates of reward seeking following protracted abstinence in mice.* J Physiol, 2012. **590**(Pt 10): p. 2427-42.
179. Maldjian, J.A., P.J. Laurienti, R.A. Kraft, and J.H. Burdette, *An automated method for neuroanatomic and cytoarchitectonic atlas-based interrogation of fMRI data sets.* Neuroimage, 2003. **19**(3): p. 1233-9.
180. Maldjian, J.A., P.J. Laurienti, and J.H. Burdette, *Precentral gyrus discrepancy in electronic versions of the Talairach atlas.* Neuroimage, 2004. **21**(1): p. 450-5.
181. Martin, L.J., R.E. Powers, T.L. Dellovade, and D.L. Price, *The bed nucleus-amygdala continuum in human and monkey.* J Comp Neurol, 1991. **309**(4): p. 445-85.
182. Masugi, F., T. Ogihara, K. Sakaguchi, A. Otsuka, Y. Tsuchiya, S. Morimoto, Y. Kumahara, S. Saeki, and M. Nishide, *High plasma levels of cortisol in patients with senile dementia of the Alzheimer's type.* Methods Find Exp Clin Pharmacol, 1989. **11**(11): p. 707-10.

183. Masuhr, K.F. and M. Neumann, *Degenerative (atrophische) Prozesse des Gehirns und Rückenmarks*, in *Neurologie*. 2007, Thieme Verlag KG: Stuttgart. p. 191-237.
184. McDonald, A.J., *Neurons of the bed nucleus of the stria terminalis: a golgi study in the rat.* Brain Res Bull, 1983. **10**(1): p. 111-20.
185. McDonald, A.J., S.J. Shammah-Lagnado, C. Shi, and M. Davis, *Cortical afferents to the extended amygdala.* Ann N Y Acad Sci, 1999. **877**: p. 309-38.
186. Merboldt, K.D., W. Hanicke, and J. Frahm, *Self-Diffusion Nmr Imaging Using Stimulated Echoes.* Journal of Magnetic Resonance, 1985. **64**(3): p. 479-486.
187. Michael, R.P. and E.B. Keverne, *Pheromones in the communication of sexual status in primates.* Nature, 1968. **218**(5143): p. 746-9.
188. Miller, M.A., L. Vician, D.K. Clifton, and D.M. Dorsa, *Sex differences in vasopressin neurons in the bed nucleus of the stria terminalis by in situ hybridization.* Peptides, 1989. **10**(3): p. 615-9.
189. Minthon, L., L. Edvinsson, and L. Gustafson, *Correlation between clinical characteristics and cerebrospinal fluid neuropeptide Y levels in dementia of the Alzheimer type and frontotemporal dementia.* Alzheimer Dis Assoc Disord, 1996. **10**(4): p. 197-203.
190. Mobbs, D., R. Yu, J.B. Rowe, H. Eich, O. FeldmanHall, and T. Dalgleish, *Neural activity associated with monitoring the oscillating threat value of a tarantula.* Proc Natl Acad Sci U S A, 2010. **107**(47): p. 20582-6.
191. Moga, M.M., C.B. Saper, and T.S. Gray, *Bed nucleus of the stria terminalis: cytoarchitecture, immunohistochemistry, and projection to the parabrachial nucleus in the rat.* J Comp Neurol, 1989. **283**(3): p. 315-32.
192. Moga, M.M. and C.B. Saper, *Neuropeptide-immunoreactive neurons projecting to the paraventricular hypothalamic nucleus in the rat.* J Comp Neurol, 1994. **346**(1): p. 137-50.
193. Mohammadi, S., H.E. Moller, H. Kugel, D.K. Muller, and M. Deppe, *Correcting eddy current and motion effects by affine whole-brain registrations: evaluation of three-dimensional distortions and comparison with slicewise correction.* Magn Reson Med, 2010. **64**(4): p. 1047-56.
194. Morano, T.J., N.J. Bailey, C.M. Cahill, and E.C. Dumont, *Nuclei-and condition-specific responses to pain in the bed nucleus of the stria terminalis.* Prog Neuropsychopharmacol Biol Psychiatry, 2008. **32**(3): p. 643-50.
195. Mori, S. and P.C. van Zijl, *Fiber tracking: principles and strategies - a technical review.* NMR Biomed, 2002. **15**(7-8): p. 468-80.
196. Motzkin, J.C., C.L. Philippi, J.A. Oler, N.H. Kalin, M.K. Baskaya, and M. Koenigs, *Ventromedial prefrontal cortex damage alters resting blood flow to the bed nucleus of stria terminalis.* Cortex, 2014. **64**: p. 281-288.
197. Mulisch, M. and U.E. Welsch, *Romeis - Mikroskopische Technik*. 18 ed. 2010, Heidelberg: Spektrum Akademischer Verlag.
198. Myers, B., C. Mark Dolgas, J. Kasckow, W.E. Cullinan, and J.P. Herman, *Central stress-integrative circuits: forebrain glutamatergic and GABAergic projections to the dorsomedial hypothalamus, medial preoptic area, and bed nucleus of the stria terminalis.* Brain Struct Funct, 2013.

199. Naka, T., S. Ide, T. Nakako, M. Hirata, Y. Majima, S. Deyama, H. Takeda, M. Yoshioka, and M. Minami, *Activation of beta-adrenoceptors in the bed nucleus of the stria terminalis induces food intake reduction and anxiety-like behaviors.* Neuropharmacology, 2013. **67**: p. 326-30.
200. Nakagawa, T., R. Yamamoto, M. Fujio, Y. Suzuki, M. Minami, M. Satoh, and S. Kaneko, *Involvement of the bed nucleus of the stria terminalis activated by the central nucleus of the amygdala in the negative affective component of morphine withdrawal in rats.* Neuroscience, 2005. **134**(1): p. 9-19.
201. Nakanishi, H., *Microglial functions and proteases.* Mol Neurobiol, 2003. **27**(2): p. 163-76.
202. Naqvi, N.H., D. Rudrauf, H. Damasio, and A. Bechara, *Damage to the insula disrupts addiction to cigarette smoking.* Science, 2007. **315**(5811): p. 531-4.
203. Norris, D.G., *Implications of bulk motion for diffusion-weighted imaging experiments: effects, mechanisms, and solutions.* J Magn Reson Imaging, 2001. **13**(4): p. 486-95.
204. Novotny, G.E., *A direct ventral connection between the bed nucleus of the stria terminalis and the amygdaloid complex in the monkey (Macaca fascicularis).* J Hirnforsch, 1977. **18**(3): p. 271-84.
205. Oldfield, R.C., *The assessment and analysis of handedness: the Edinburgh inventory.* Neuropsychologia, 1971. **9**(1): p. 97-113.
206. Oler, J.A., A.S. Fox, S.E. Shelton, B.T. Christian, D. Murali, T.R. Oakes, R.J. Davidson, and N.H. Kalin, *Serotonin transporter availability in the amygdala and bed nucleus of the stria terminalis predicts anxious temperament and brain glucose metabolic activity.* J Neurosci, 2009. **29**(32): p. 9961-6.
207. Oler, J.A., R.M. Birn, R. Patriat, A.S. Fox, S.E. Shelton, C.A. Burghy, D.E. Stodola, M.J. Essex, R.J. Davidson, and N.H. Kalin, *Evidence for coordinated functional activity within the extended amygdala of non-human and human primates.* Neuroimage, 2012. **61**(4): p. 1059-66.
208. Olive, M.F., H.N. Koenig, M.A. Nannini, and C.W. Hodge, *Elevated extracellular CRF levels in the bed nucleus of the stria terminalis during ethanol withdrawal and reduction by subsequent ethanol intake.* Pharmacol Biochem Behav, 2002. **72**(1-2): p. 213-20.
209. Page, K.J., L. Potter, S. Aronni, B.J. Everitt, and S.B. Dunnett, *The expression of Huntingtin-associated protein (HAP1) mRNA in developing, adult and ageing rat CNS: implications for Huntington's disease neuropathology.* Eur J Neurosci, 1998. **10**(5): p. 1835-45.
210. Park, J., R.A. Wheeler, K. Fontillas, R.B. Keithley, R.M. Carelli, and R.M. Wightman, *Catecholamines in the bed nucleus of the stria terminalis reciprocally respond to reward and aversion.* Biol Psychiatry, 2012. **71**(4): p. 327-34.
211. Park, J., E.S. Bucher, K. Fontillas, C. Owesson-White, J.L. Ariansen, R.M. Carelli, and R.M. Wightman, *Opposing catecholamine changes in the bed nucleus of the stria terminalis during intracranial self-stimulation and its extinction.* Biol Psychiatry, 2013. **74**(1): p. 69-76.

212. Paxinos, G., *Interruption of septal connections: effects on drinking, irritability, and copulation.* Physiol Behav, 1976. **17**(1): p. 81-8.
213. Poletti, C.E., M. Kliot, and M. Boytim, *Metabolic influence of the hippocampus on hypothalamus, preoptic and basal forebrain is exerted through amygdalofugal pathways.* Neurosci Lett, 1984. **45**(2): p. 211-6.
214. Politis, M., N. Pavese, Y.F. Tai, L. Kiferle, S.L. Mason, D.J. Brooks, S.J. Tabrizi, R.A. Barker, and P. Piccini, *Microglial activation in regions related to cognitive function predicts disease onset in Huntington's disease: a multimodal imaging study.* Hum Brain Mapp, 2011. **32**(2): p. 258-70.
215. Powers, J.B. and S.S. Winans, *Vomeronasal organ: critical role in mediating sexual behavior of the male hamster.* Science, 1975. **187**(4180): p. 961-3.
216. Prewitt, C.M. and J.P. Herman, *Anatomical interactions between the central amygdaloid nucleus and the hypothalamic paraventricular nucleus of the rat: a dual tract-tracing analysis.* J Chem Neuroanat, 1998. **15**(3): p. 173-85.
217. Radke, A.K. and J.C. Gewirtz, *Increased dopamine receptor activity in the nucleus accumbens shell ameliorates anxiety during drug withdrawal.* Neuropsychopharmacology, 2012. **37**(11): p. 2405-15.
218. Radley, J.J., K.L. Gosselink, and P.E. Sawchenko, *A discrete GABAergic relay mediates medial prefrontal cortical inhibition of the neuroendocrine stress response.* J Neurosci, 2009. **29**(22): p. 7330-40.
219. Reep, R.L. and S.S. Winans, *Afferent connections of dorsal and ventral agranular insular cortex in the hamster Mesocricetus auratus.* Neuroscience, 1982. **7**(5): p. 1265-88.
220. Ricardo, J.A. and E.T. Koh, *Anatomical evidence of direct projections from the nucleus of the solitary tract to the hypothalamus, amygdala, and other forebrain structures in the rat.* Brain Res, 1978. **153**(1): p. 1-26.
221. Rivalland, E.T., A.J. Tilbrook, A.I. Turner, J. Iqbal, S. Pompolo, and I.J. Clarke, *Projections to the preoptic area from the paraventricular nucleus, arcuate nucleus and the bed nucleus of the stria terminalis are unlikely to be involved in stress-induced suppression of GnRH secretion in sheep.* Neuroendocrinology, 2006. **84**(1): p. 1-13.
222. Roberts, G.W., P.L. Woodhams, J.M. Polak, and T.J. Crow, *Distribution of neuropeptides in the limbic system of the rat: the amygdaloid complex.* Neuroscience, 1982. **7**(1): p. 99-131.
223. Roman, C., N. Nebieridze, A. Sastre, and S. Reilly, *Effects of lesions of the bed nucleus of the stria terminalis, lateral hypothalamus, or insular cortex on conditioned taste aversion and conditioned odor aversion.* Behav Neurosci, 2006. **120**(6): p. 1257-67.
224. Rouwette, T., P. Vanelderen, M. de Reus, N.O. Loohuis, J. Giele, J. van Egmond, W. Scheenen, G.J. Scheffer, E. Roubos, K. Vissers, and T. Kozicz, *Experimental neuropathy increases limbic forebrain CRF.* Eur J Pain, 2012. **16**(1): p. 61-71.
225. Russell, G.V., E.S. Barratt, J.M. Deaton, and R.R. Taylor, Jr., *Evoked responses in the putamen and globus pallidus following stimulation o f the basolateral amygdala.* Brain Res, 1968. **7**(3): p. 459-62.

226. Rygula, R., H.F. Clarke, R.N. Cardinal, G.J. Cockcroft, J. Xia, J.W. Dalley, T.W. Robbins, and A.C. Roberts, *Role of Central Serotonin in Anticipation of Rewarding and Punishing Outcomes: Effects of Selective Amygdala or Orbitofrontal 5-HT Depletion.* Cereb Cortex, 2014.
227. Sajdyk, T., P. Johnson, S. Fitz, and A. Shekhar, *Chronic inhibition of GABA synthesis in the bed nucleus of the stria terminalis elicits anxiety-like behavior.* J Psychopharmacol, 2008. **22**(6): p. 633-41.
228. Sanides, F., *Die Insulae terminales des Erwachsenengehirns des Menschen.* J Hirnforsch, 1957. **3**(2-3): p. 243-73.
229. Saper, C.B. and A.D. Loewy, *Efferent connections of the parabrachial nucleus in the rat.* Brain Res, 1980. **197**(2): p. 291-317.
230. Saper, C.B., *Convergence of autonomic and limbic connections in the insular cortex of the rat.* J Comp Neurol, 1982. **210**(2): p. 163-73.
231. Saphier, D. and S. Feldman, *Electrophysiology of limbic forebrain and paraventricular nucleus connections.* Brain Res Bull, 1986. **17**(6): p. 743-50.
232. Sartor, G.C. and G. Aston-Jones, *Regulation of the ventral tegmental area by the bed nucleus of the stria terminalis is required for expression of cocaine preference.* Eur J Neurosci, 2012. **36**(11): p. 3549-58.
233. Sawchenko, P.E. and L.W. Swanson, *The organization of forebrain afferents to the paraventricular and supraoptic nuclei of the rat.* J Comp Neurol, 1983. **218**(2): p. 121-44.
234. Sawchenko, P.E., E.R. Brown, R.K. Chan, A. Ericsson, H.Y. Li, B.L. Roland, and K.J. Kovacs, *The paraventricular nucleus of the hypothalamus and the functional neuroanatomy of visceromotor responses to stress.* Prog Brain Res, 1996. **107**: p. 201-22.
235. Schlund, M.W., C.D. Hudgins, S. Magee, and S. Dymond, *Neuroimaging the temporal dynamics of human avoidance to sustained threat.* Behav Brain Res, 2013. **257**: p. 148-55.
236. Schmuckermair, C., S. Gaburro, A. Sah, R. Landgraf, S.B. Sartori, and N. Singewald, *Behavioral and neurobiological effects of deep brain stimulation in a mouse model of high anxiety- and depression-like behavior.* Neuropsychopharmacology, 2013. **38**(7): p. 1234-44.
237. Shaham, Y., S. Erb, and J. Stewart, *Stress-induced relapse to heroin and cocaine seeking in rats: a review.* Brain Res Brain Res Rev, 2000. **33**(1): p. 13-33.
238. Shammah-Lagnado, S.J., G.F. Alheid, and L. Heimer, *Afferent connections of the interstitial nucleus of the posterior limb of the anterior commissure and adjacent amygdalostriatal transition area in the rat.* Neuroscience, 1999. **94**(4): p. 1097-123.
239. Shimony, J.S., R.C. McKinstry, E. Akbudak, J.A. Aronovitz, A.Z. Snyder, N.F. Lori, T.S. Cull, and T.E. Conturo, *Quantitative diffusion-tensor anisotropy brain MR imaging: normative human data and anatomic analysis.* Radiology, 1999. **212**(3): p. 770-84.
240. Shin, J.W., J.C. Geerling, and A.D. Loewy, *Inputs to the ventrolateral bed nucleus of the stria terminalis.* J Comp Neurol, 2008. **511**(5): p. 628-57.

241. Shinohara, K., M. Morofushi, T. Funabashi, and F. Kimura, *Axillary pheromones modulate pulsatile LH secretion in humans.* Neuroreport, 2001. **12**(5): p. 893-5.
242. Shrager, R.I. and P.J. Basser, *Anisotropically weighted MRI.* Magn Reson Med, 1998. **40**(1): p. 160-5.
243. Silberman, Y., R.T. Matthews, and D.G. Winder, *A corticotropin releasing factor pathway for ethanol regulation of the ventral tegmental area in the bed nucleus of the stria terminalis.* J Neurosci, 2013. **33**(3): p. 950-60.
244. Simerly, R.B., C. Chang, M. Muramatsu, and L.W. Swanson, *Distribution of androgen and estrogen receptor mRNA-containing cells in the rat brain: an in situ hybridization study.* J Comp Neurol, 1990. **294**(1): p. 76-95.
245. Sladky, R., A. Hoflich, M. Kublbock, C. Kraus, P. Baldinger, E. Moser, R. Lanzenberger, and C. Windischberger, *Disrupted Effective Connectivity Between the Amygdala and Orbitofrontal Cortex in Social Anxiety Disorder During Emotion Discrimination Revealed by Dynamic Causal Modeling for fMRI.* Cereb Cortex, 2015. **25**(4): p. 895-903.
246. Somerville, L.H., P.J. Whalen, and W.M. Kelley, *Human bed nucleus of the stria terminalis indexes hypervigilant threat monitoring.* Biol Psychiatry, 2010. **68**(5): p. 416-24.
247. Somerville, L.H., D.D. Wagner, G.S. Wig, J.M. Moran, P.J. Whalen, and W.M. Kelley, *Interactions between transient and sustained neural signals support the generation and regulation of anxious emotion.* Cereb Cortex, 2013. **23**(1): p. 49-60.
248. Spencer, S.J., K.M. Buller, and T.A. Day, *Medial prefrontal cortex control of the paraventricular hypothalamic nucleus response to psychological stress: possible role of the bed nucleus of the stria terminalis.* J Comp Neurol, 2005. **481**(4): p. 363-76.
249. Stejskal, E.O. and J.E. Tanner, *Spin Diffusion Measurements: Spin Echoes in the Presence of a Time-Dependent Field Gradient.* Journal of Chemical Physics, 1965. **42**(1): p. 288-+.
250. Stern, K. and M.K. McClintock, *Regulation of ovulation by human pheromones.* Nature, 1998. **392**(6672): p. 177-9.
251. Stieltjes, B., W.E. Kaufmann, P.C. van Zijl, K. Fredericksen, G.D. Pearlson, M. Solaiyappan, and S. Mori, *Diffusion tensor imaging and axonal tracking in the human brainstem.* Neuroimage, 2001. **14**(3): p. 723-35.
252. Stinus, L., M. Cador, E.P. Zorrilla, and G.F. Koob, *Buprenorphine and a CRF1 antagonist block the acquisition of opiate withdrawal-induced conditioned place aversion in rats.* Neuropsychopharmacology, 2005. **30**(1): p. 90-8.
253. Straube, T., H.J. Mentzel, and W.H. Miltner, *Waiting for spiders: brain activation during anticipatory anxiety in spider phobics.* Neuroimage, 2007. **37**(4): p. 1427-36.
254. Sullivan, G.M., J. Apergis, D.E. Bush, L.R. Johnson, M. Hou, and J.E. Ledoux, *Lesions in the bed nucleus of the stria terminalis disrupt corticosterone and freezing responses elicited by a contextual but not by a specific cue-conditioned fear stimulus.* Neuroscience, 2004. **128**(1): p. 7-14.

255. Sun, W., C.K. Akins, A.E. Mattingly, and G.V. Rebec, *Ionotropic glutamate receptors in the ventral tegmental area regulate cocaine-seeking behavior in rats.* Neuropsychopharmacology, 2005. **30**(11): p. 2073-81.
256. Swaab, D.F. and M.A. Hofman, *Sexual differentiation of the human hypothalamus: ontogeny of the sexually dimorphic nucleus of the preoptic area.* Brain Res Dev Brain Res, 1988. **44**(2): p. 314-8.
257. Swaab, D.F., *The Human Hypothalamus: Basic and Clinical Aspects, Part I: Nuclei of the Human Hypothalamus*, in *Handb Clin Neurol*. 2003, Elsevier B. V.: Amsterdam; Boston. p. 61-62.
258. Swann, J.M., J. Wang, and E.K. Govek, *The MPN mag: introducing a critical area mediating pheromonal and hormonal regulation of male sexual behavior.* Ann N Y Acad Sci, 2003. **1007**: p. 199-210.
259. Swanson, L.W., *An autoradiographic study of the efferent connections of the preoptic region in the rat.* J Comp Neurol, 1976. **167**(2): p. 227-56.
260. Takagishi, M. and T. Chiba, *Efferent projections of the infralimbic (area 25) region of the medial prefrontal cortex in the rat: an anterograde tracer PHA-L study.* Brain Res, 1991. **566**(1-2): p. 26-39.
261. Taylor, D.G. and M.C. Bushell, *The Spatial-Mapping of Translational Diffusion-Coefficients by the Nmr Imaging Technique.* Physics in Medicine and Biology, 1985. **30**(4): p. 345-349.
262. Techavipoo, U., J. Lackey, J. Shi, X. Guan, and S. Lai, *Estimation of mutual information objective function based on Fourier shift theorem: an application to eddy current distortion correction in diffusion tensor imaging.* Magn Reson Imaging, 2009. **27**(9): p. 1281-92.
263. Tournier, J.D., F. Calamante, D.G. Gadian, and A. Connelly, *Direct estimation of the fiber orientation density function from diffusion-weighted MRI data using spherical deconvolution.* Neuroimage, 2004. **23**(3): p. 1176-85.
264. Tournier, J.D., F. Calamante, and A. Connelly, *Robust determination of the fibre orientation distribution in diffusion MRI: non-negativity constrained super-resolved spherical deconvolution.* Neuroimage, 2007. **35**(4): p. 1459-72.
265. Tuch, D.S., *Q-ball imaging.* Magn Reson Med, 2004. **52**(6): p. 1358-72.
266. Turner, R., D. Le Bihan, J. Maier, R. Vavrek, L.K. Hedges, and J. Pekar, *Echo-planar imaging of intravoxel incoherent motion.* Radiology, 1990. **177**(2): p. 407-14.
267. Turner, R., D. Le Bihan, and A.S. Chesnick, *Echo-planar imaging of diffusion and perfusion.* Magn Reson Med, 1991. **19**(2): p. 247-53.
268. Uylings, H.B. and C.G. van Eden, *Qualitative and quantitative comparison of the prefrontal cortex in rat and in primates, including humans.* Prog Brain Res, 1990. **85**: p. 31-62.
269. Valcourt, R.J. and B.D. Sachs, *Penile reflexes and copulatory behavior in male rats following lesions in the bed nucleus of the stria terminalis.* Brain Res Bull, 1979. **4**(1): p. 131-3.
270. Van Eden, C.G. and R.M. Buijs, *Functional neuroanatomy of the prefrontal cortex: autonomic interactions.* Prog Brain Res, 2000. **126**: p. 49-62.

271. van Leeuwen, F. and R. Caffe, *Vasopressin-immunoreactive cell bodies in the bed nucleus of the stria terminalis of the rat.* Cell Tissue Res, 1983. **228**(3): p. 525-34.
272. van Leeuwen, F.W., A.R. Caffe, and G.J. De Vries, *Vasopressin cells in the bed nucleus of the stria terminalis of the rat: sex differences and the influence of androgens.* Brain Res, 1985. **325**(1-2): p. 391-4.
273. Vertes, R.P., *Differential projections of the infralimbic and prelimbic cortex in the rat.* Synapse, 2004. **51**(1): p. 32-58.
274. Vertes, R.P. and W.B. Hoover, *Projections of the paraventricular and paratenial nuclei of the dorsal midline thalamus in the rat.* J Comp Neurol, 2008. **508**(2): p. 212-37.
275. Vos, S.B., M.A. Viergever, and A. Leemans, *Multi-fiber tractography visualizations for diffusion MRI data.* PLoS One, 2013. **8**(11): p. e81453.
276. Walker, D.L. and M. Davis, *Anxiogenic effects of high illumination levels assessed with the acoustic startle response in rats.* Biol Psychiatry, 1997. **42**(6): p. 461-71.
277. Walker, D.L. and M. Davis, *Double dissociation between the involvement of the bed nucleus of the stria terminalis and the central nucleus of the amygdala in startle increases produced by conditioned versus unconditioned fear.* J Neurosci, 1997. **17**(23): p. 9375-83.
278. Walker, D.L. and M. Davis, *Role of the extended amygdala in short-duration versus sustained fear: a tribute to Dr. Lennart Heimer.* Brain Struct Funct, 2008. **213**(1-2): p. 29-42.
279. Walker, D.L., L.A. Miles, and M. Davis, *Selective participation of the bed nucleus of the stria terminalis and CRF in sustained anxiety-like versus phasic fear-like responses.* Prog Neuropsychopharmacol Biol Psychiatry, 2009. **33**(8): p. 1291-308.
280. Walter, A., J.K. Mai, L. Lanta, and T. Gorcs, *Differential distribution of immunohistochemical markers in the bed nucleus of the stria terminalis in the human brain.* J Chem Neuroanat, 1991. **4**(4): p. 281-98.
281. Wang, J., C. Chang, N. Geng, X. Wang, and G. Gao, *Treatment of intractable anorexia nervosa with inactivation of the nucleus accumbens using stereotactic surgery.* Stereotact Funct Neurosurg, 2013. **91**(6): p. 364-72.
282. Wedeen, V.J., P. Hagmann, W.Y. Tseng, T.G. Reese, and R.M. Weisskoff, *Mapping complex tissue architecture with diffusion spectrum magnetic resonance imaging.* Magn Reson Med, 2005. **54**(6): p. 1377-86.
283. Weishaupt, D., V.D. Köchli, and B. Marincek, *Wie funktioniert MRI?* 6. ed. 2009, Heidelberg: Springer.
284. Weller, K.L. and D.A. Smith, *Afferent connections to the bed nucleus of the stria terminalis.* Brain Res, 1982. **232**(2): p. 255-70.
285. Weller, L. and A. Weller, *Human menstrual synchrony: a critical assessment.* Neurosci Biobehav Rev, 1993. **17**(4): p. 427-39.
286. Whitnall, M.H., *Regulation of the hypothalamic corticotropin-releasing hormone neurosecretory system.* Prog Neurobiol, 1993. **40**(5): p. 573-629.
287. Winans, S.S. and J.B. Powers, *Olfactory and vomeronasal deafferentation of male hamsters: histological and behavioral analyses.* Brain Res, 1977. **126**(2): p. 325-44.

288. Woodhams, P.L., G.W. Roberts, J.M. Polak, and T.J. Crow, *Distribution of neuropeptides in the limbic system of the rat: the bed nucleus of the stria terminalis, septum and preoptic area.* Neuroscience, 1983. **8**(4): p. 677-703.
289. Xu, D., J.K. Maier, K.F. King, B.D. Collick, G. Wu, R.D. Peters, and R.S. Hinks, *Prospective and retrospective high order eddy current mitigation for diffusion weighted echo planar imaging.* Magn Reson Med, 2013. **70**(5): p. 1293-305.
290. Xu, J. and M.N. Potenza, *White matter integrity and five-factor personality measures in healthy adults.* Neuroimage, 2012. **59**(1): p. 800-7.
291. Yassa, M.A., R.L. Hazlett, C.E. Stark, and R. Hoehn-Saric, *Functional MRI of the amygdala and bed nucleus of the stria terminalis during conditions of uncertainty in generalized anxiety disorder.* J Psychiatr Res, 2012. **46**(8): p. 1045-52.
292. Yasui, Y., C.D. Breder, C.B. Saper, and D.F. Cechetto, *Autonomic responses and efferent pathways from the insular cortex in the rat.* J Comp Neurol, 1991. **303**(3): p. 355-74.
293. Zhou, J.N., M.A. Hofman, L.J. Gooren, and D.F. Swaab, *A sex difference in the human brain and its relation to transsexuality.* Nature, 1995. **378**(6552): p. 68-70.
294. Zhuang, J., J. Hrabe, A. Kangarlu, D. Xu, R. Bansal, C.A. Branch, and B.S. Peterson, *Correction of eddy-current distortions in diffusion tensor images using the known directions and strengths of diffusion gradients.* J Magn Reson Imaging, 2006. **24**(5): p. 1188-93.

Erklärung zum Eigenanteil

Oliver Krüger

Hiermit erkläre ich, dass ich die beigefügte Dissertation selbstständig verfasst und keine anderen als die angegebenen Hilfsmittel genutzt habe. Ich versichere, die den Ergebnissen dieser Arbeit zugrunde liegenden Experimente, mit u. g. Ausnahmen, eigenverantwortlich durchgeführt und ausgewertet zu haben und die den theoretischen Abschnitten dieser Arbeit zugrunde liegende Literaturrecherche selbst durchgeführt zu haben. Alle wörtlich oder inhaltlich übernommenen Stellen habe ich als solche gekennzeichnet.

Herr Professor Dr. med. Thomas Ethofer war an der Konzeption der Studie beteiligt, er hat die Arbeit betreut und das Manuskript korrigiert.
Herr Dr. med. Thomas Shiozawa hat die in dieser Arbeit beschriebenen histologischen Kontrollexperimente auf meine Veranlassung hin durchgeführt und die Unterkapitel *3.4 Specimen for Histological Control Experiment* sowie *3.5 Microscopic Slides* zu großen Teilen verfasst.

Ich versichere außerdem, dass ich die beigefügte Dissertation nur in diesem und keinem anderen Promotionsverfahren eingereicht habe und dass diesem Promotionsverfahren keine endgültig gescheiterten Promotionsverfahren vorausgegangen sind.

_____ _____

Ort, Datum Unterschrift

Veröffentlichungen

Teile der vorliegenden Dissertationsschrift wurden bereits in folgender Publikation veröffentlich:

Krüger, O., Shiozawa, T., Kreifelts, B., Scheffler, K., Ethofer, T. – Three distinct fiber pathways of the bed nucleus of the stria terminalis to the amygdala and prefrontal cortex – Cortex – 2015 – Band 66 – S. 60-68.